Development of Novel Germanium Detectors for Rare Event Physics Searches

Wenzhao Wei on behalf of the HPGe detector development group at USD

University of South Dakota

May 13, 2022

CoSSURF 2022

PIRE GEMADARC

UNIVERSITY OF SOUTH DAKOTA

Motivation (Physics)

- Germanium (Ge) is a leading material in the direct detection of low-mass dark matter and neutrinoless double-beta ($0\nu\beta\beta$) decay.
- Also, Ge has great potential to improve the sensitivity of neutrino experiments including coherent elastic neutrino-nucleus scattering (CEνNS). This is because Ge has the following advantages[1]:
  - Commercial availability of large detector volumes (10 cm diameter boules)
  - Ability to fully deplete thick detector layers (a few cm)
  - Relatively high atomic number

  → High detection efficiency
  - Near-perfect charge collection
  - Favorable charge generation statistics

  → Excellent energy resolution

Low-Mass Dark Matter Searches

- Extremely low energy threshold is required to detect MeV-scale dark matter. Ge-based SuperCDMS experiment can achieve the lowest threshold (~50 eV) of any dark matter experiment so far[2].

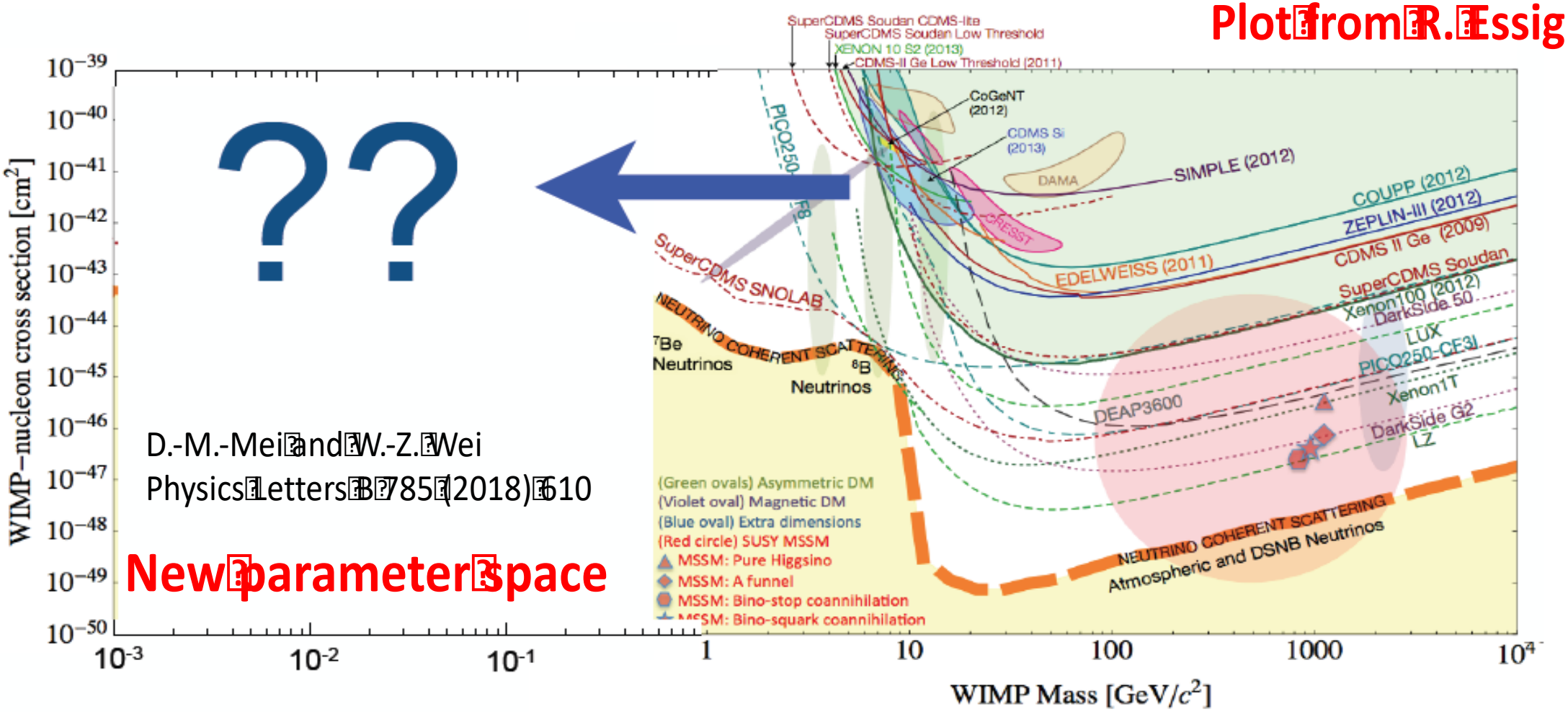

$0\nu\beta\beta$ Decay

- Ge detectors achieve the best energy resolution of any $0\nu\beta\beta$ decay experiment, while also providing detailed information on the event topology[3].
- ^{76}Ge-based experiments, GERDA and MAJORANA DEMONSTRATOR, have achieved the lowest background of any $0\nu\beta\beta$ decay experiment when normalized to energy resolution and operate in a quasi-background-free regime[3].

Experiment	Isotope	Exposure[kg-yr]	$T_{1/2}^{0\nu}[10^{25}yr]$	$m_{\beta\beta}[\mathrm{meV}]$
GERDA	^{76}Ge	127.2	18	79 – 180
MAJORANA	^{76}Ge	26	2.7	200 – 433
KamLAND-Zen	^{136}Xe	594	10.7	61 – 165
EXO-200	^{136}Xe	234.1	3.5	93 – 286
CUORE	^{130}Te	1038.4	2.2	90 – 305

Comparison of lower half-life limits $T_{1/2}^{0\nu}$ (90% CL) and corresponding upper Majorana neutrino mass $m_{\beta\beta}$ limits for the present-generation experiments. The range of $m_{\beta\beta}$ upper limits are from each collaboration's choice of multiple matrix elements[3].

$$(A, Z) \rightarrow (A, Z+2) + e^- + e^-,$$

$$(T_{1/2}^{0\nu})^{-1} = G_{0\nu}\, g_A^4 \left(M_{0\nu} + \frac{g_\nu^{NN} m_\pi^2}{g_A^2} M_{0\nu}^{cont} \right)^2 m_{\beta\beta}^2$$

$$M_{0\nu} = M_{\mathrm{GT}}^{(0\nu)} - \left(\frac{g_V}{g_A}\right)^2 M_{\mathrm{F}}^{(0\nu)} + M_{\mathrm{T}}^{(0\nu)}.$$

$$m_{\beta\beta} = \left| \sum_{i=1}^{3} U_{ei}^2 m_i \right|$$

CEνNS

- Experimental signature – less than about 50 keV of energy deposited from nuclear recoil → extremely low energy threshold is required[4]. Ge-based experiment, TEXONO, can achieve the lowest threshold (~200 eV) of any CEνNS experiment[5].

$$\nu + A \rightarrow \nu + A$$

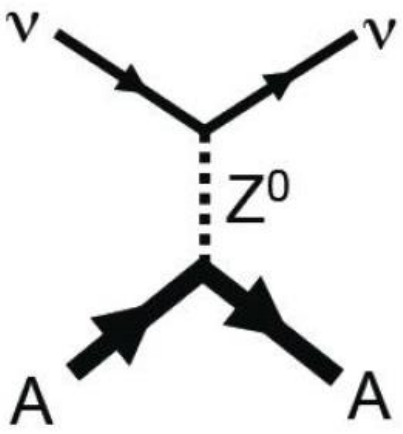

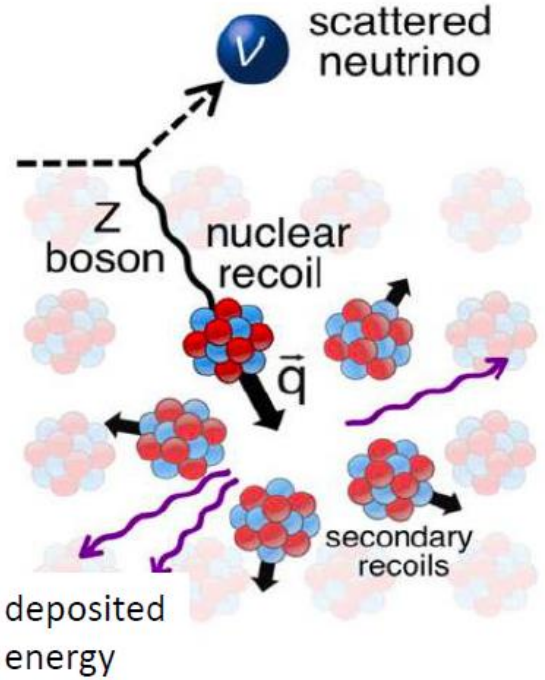

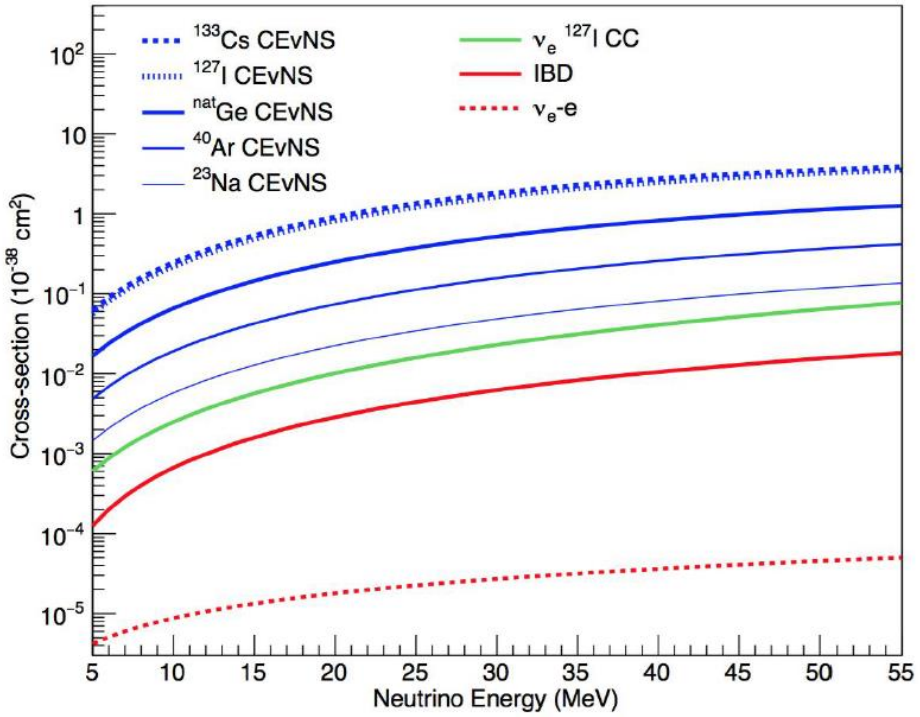

Courtesy to Diane Markoff

$$\sigma \propto Q_W^2 \propto (N - (1 - 4\sin^2\theta_W)Z)^2$$

Motivation (Technology)

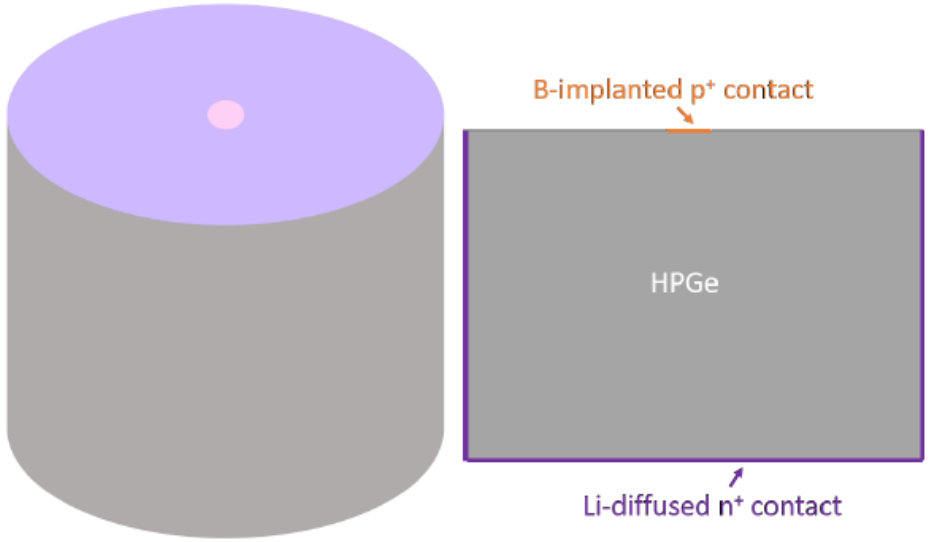

PPC-type Ge detector used by MJD[6]
(600 g to 1kg)

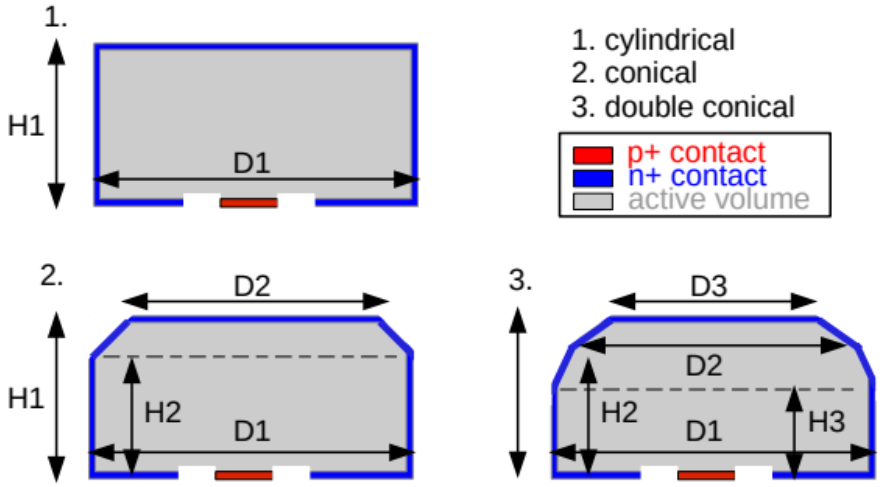

BEGe-type Ge detector used by GERDA[7]
(600 g to 1kg)

- **Advantages:** Excellent energy resolution and pulse shape discrimination (PSD) capability.
- **Disadvantage:** Cannot go larger size (> 1 kg) per detector due to the “pinch off” effect and an un-depleted region in the middle of the detector, which result in degrading energy resolution.

Motivation (Technology)

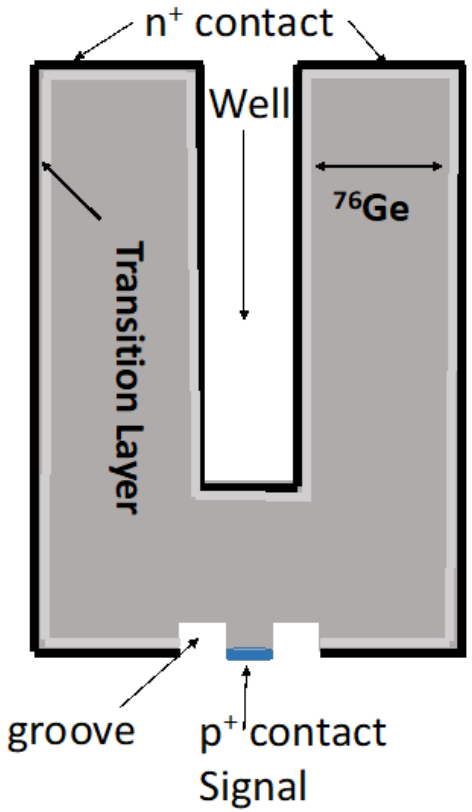

ICPC-type Ge detector
(2-3 kg)

- LEGEND-200 and LEGEND-1000 will use enriched ^{76}Ge inverted coaxial point contact (ICPC) detector, a concept invented at ORNL, that has been proven to overcome “pinch-off” for a detector with a mass of >2 kg [9].

Two issues:

- It has not been proven yet that a >4-kg detector does not have an un-depleted region in a long ICPC detector geometry.
- The n^+ contact layer (0.8 – 1 mm thick) made from Li diffusion causes the “dead” Ge (inactive in charge collection), which is the largest component of the inactive material for LEGEND-1000.

Detector Development at USD

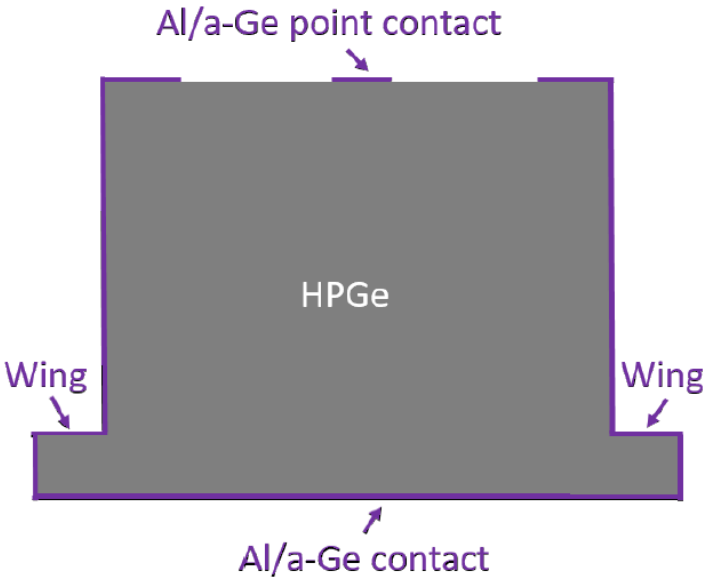

Ge Detector utilizing Internal Charge Amplification (GeICA) (shown is a planar PPC Ge detector as an example)

- Can achieve an ultra-low energy threshold of ~0.1 eV theoretically[8].

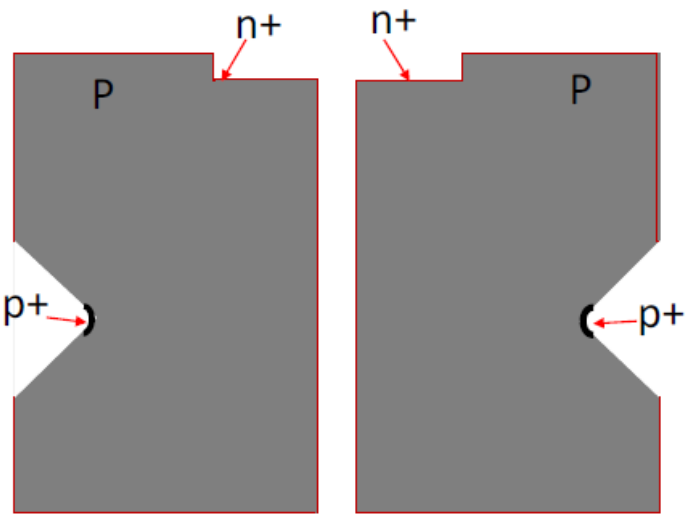

Ge Ring-Contact (GeRC) Detector (suggested by Dr. David Radford for LEGEND)

- May allow for larger crystals (>3kg) than the ICPC design.
- Expect to have similar energy resolution and PSD capability as PPC and BEGe.
- Can be fully depleted without “pinch-off” region based on Monte Carlo simulation conducted by Dr. David Radford.

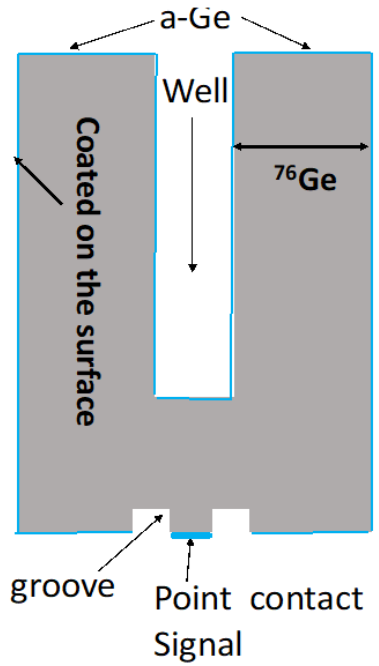

Thin-contact ICPC Ge detector

- Expect to have similar energy resolution and PSD capability as PPC and BEGe.
- Expect to largely reduce the dead Ge materials with thin contact made of a-Ge (~600 nm).

R&D of GeICA at USD

Main Research Studies

- Fabrication and characterization of planar Ge detectors at 77 K and 4 K to:
  - have a good understanding of the relationship between the fabrication process parameters and the detector performance
    - Charge barrier height of a-Ge
    - Detector performance in LAr and LN_2
    - Investigation of the electrical conduction mechanism of a-Ge
  - provide feedback to our Ge crystal growth process

- Fabrication and characterization of mini-PPC Ge detectors
  - Planar PPC
  - Cylindrical PPC

Fabrication of Planar Ge Detectors at USD

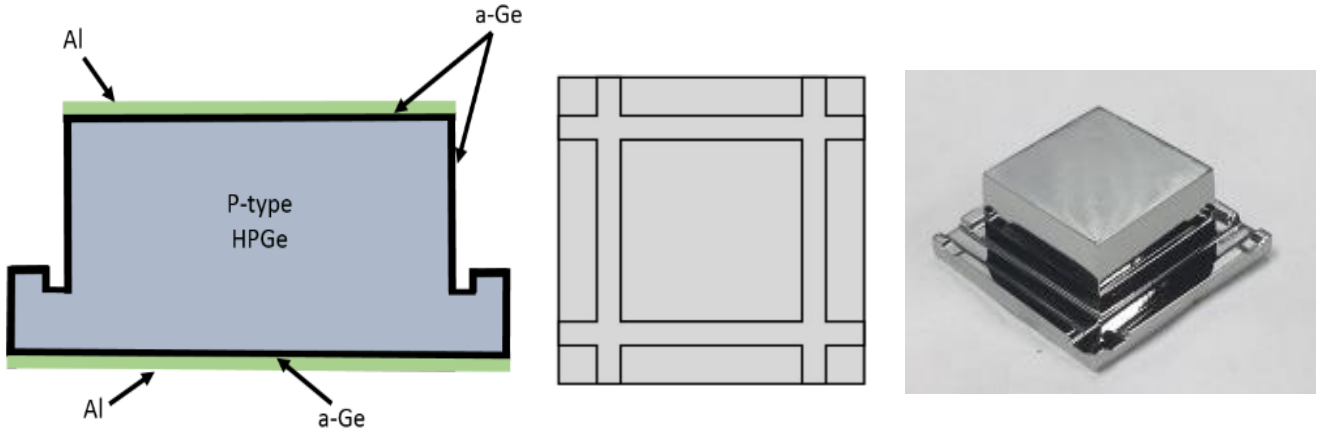

Fig.1. The typical geometry of the HPGe detectors without a guard-ring structure fabricated at USD: cross-sectional view (left), top view (middle) and the detector after chemical processing (right).

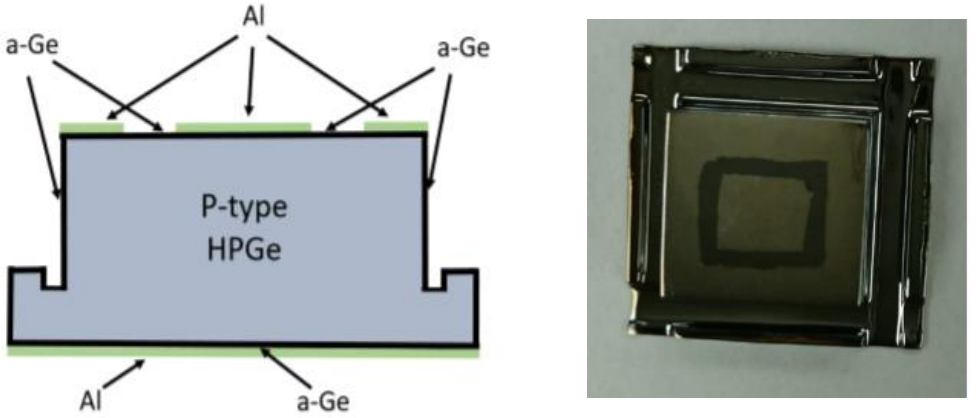

Fig.2. Left: the schematic cross-sectional view of a typical guard-ring detector fabricated at USD; Right: the top view of a guard-ring detector.

Fabrication process:

1. Mechanical processing – cut and lap to achieve desired shape and dimensions.
2. Chemical processing – etch in HNO_3:HF to remove mechanical damage and prepare surfaces for electrical contact deposition.
3. Electrical contact deposition – sputter amorphous Ge and Al to form charge carrier blocking contacts.

Detector Characterization

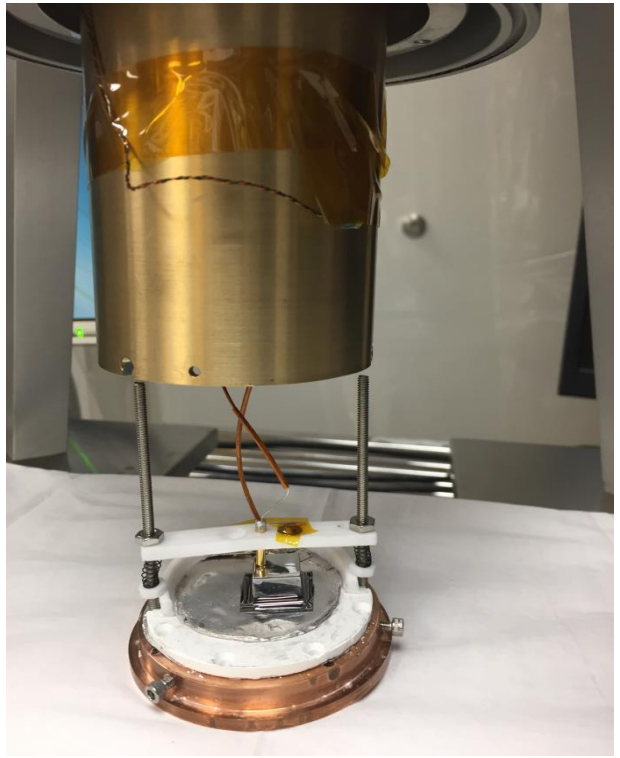

*4 K cryostat built at USD**

- I-V characteristics
- Spectroscopy measurements

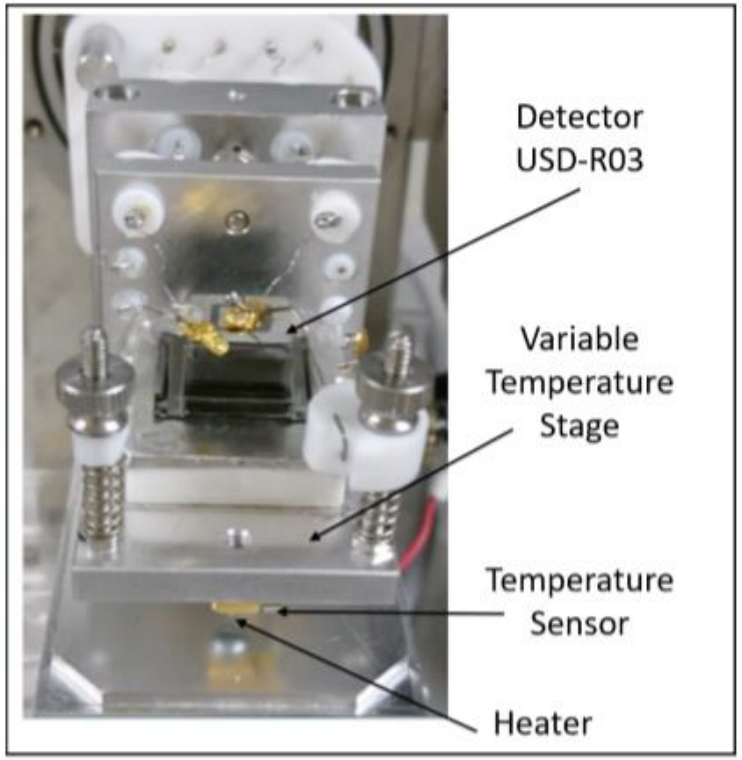

79 K cryostat from LBNL

- I-V characteristics
- C-V characteristics
- Spectroscopy measurements

** This 4 K cryostat was built by Prof. Jing Liu and graduate students at USD.*

Testing Setup at 4 K

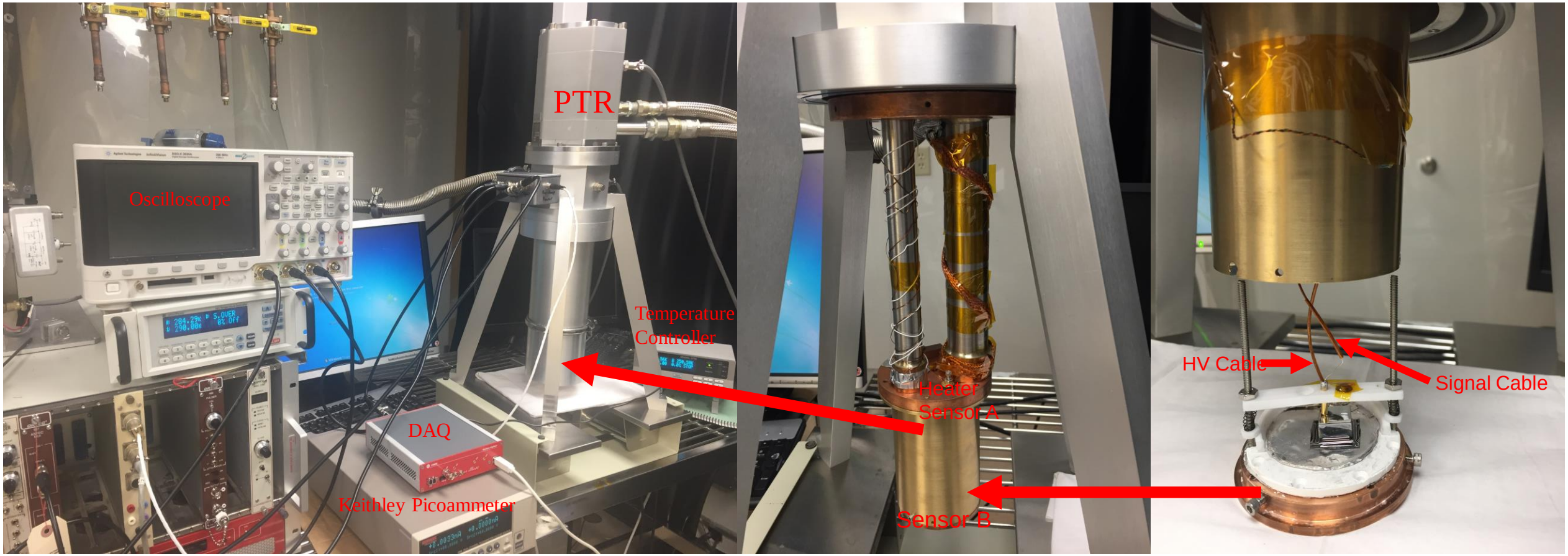

- PTR allows us to characterize the detector at liquid helium temperature, ~4 K.
- Still working on fixing some noise issues.

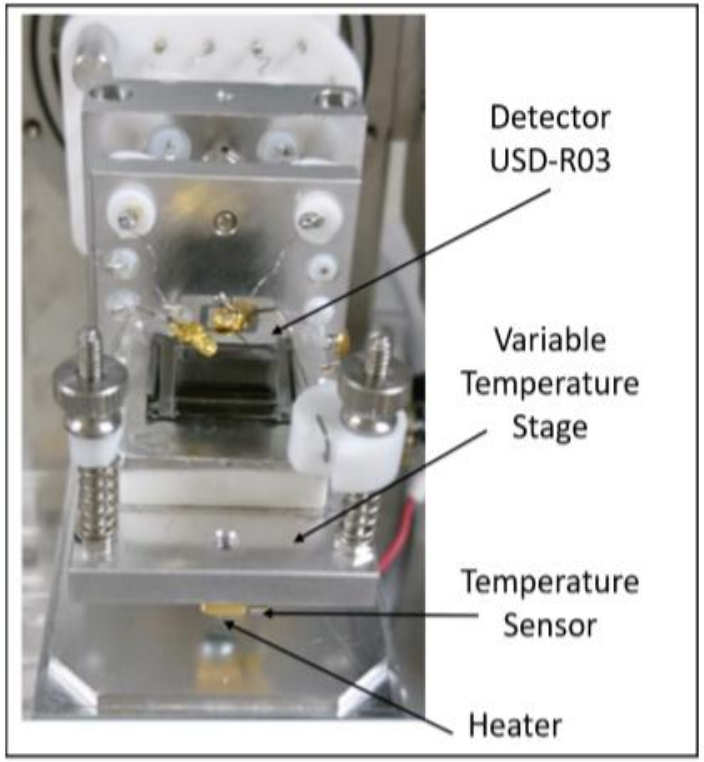

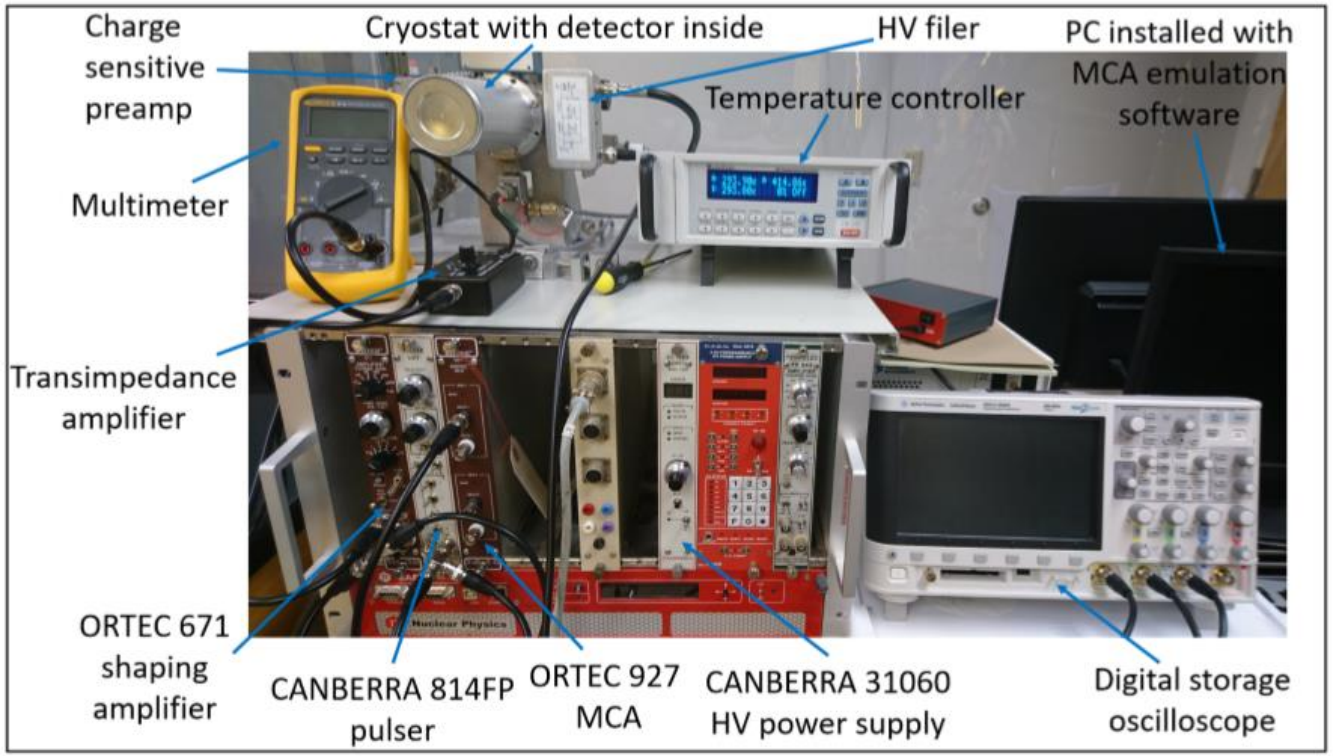

Testing Setup at 79 K

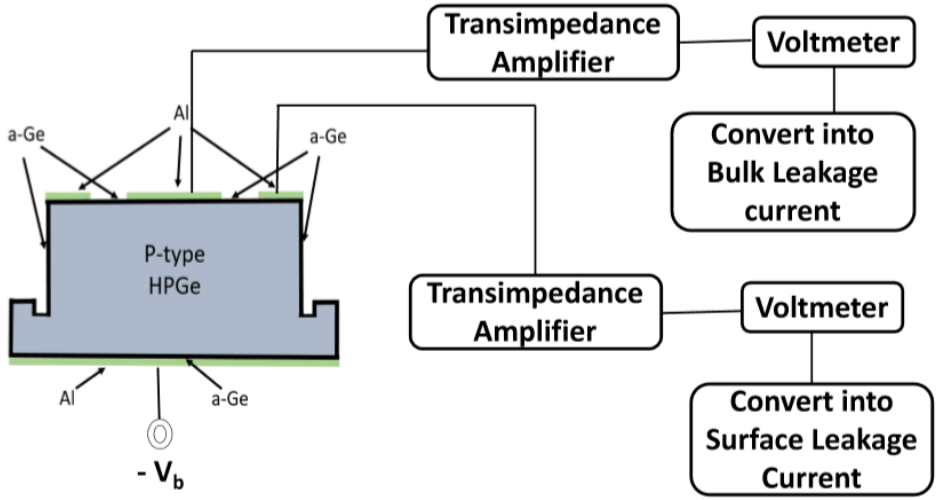

A Summary of Planar Ge Detectors Made at USD

NO.	Detectors	Fabrication Date	Crystal Number	Thickness (cm)	Active Area (cm^2)	Full Depletion Voltage (V)	Leakage Current @V_d at 79 K (pA)	N_i from C-V Measurements (/cm3)	N_i from Hall effect Measurements (/cm3)	FWHM (keV)	FWHM at Pulser Peak (keV)
1	USD-L01	12/06/2017	5-26-17A	0.54	1.31	700	1	4.25×10^{10}	$(1.5\sim1.7)\times 10^{10}$	1.57@662 keV	1.01
2	USD-L06	02/17/2018	10-23-17C	0.85	1.72	1200	1	2.94×10^{10}	$(2.6\sim4.0)\times 10^{10}$	2.22@662 keV	1.67
3	USD-L07	04/11/2018	10-23-17C	0.85	2.00	1000	1	2.45×10^{10}	$(2.6\sim4.0)\times 10^{10}$	1.59@662 keV	1.19
4	USD-L08	04/05/2018	10-23-17C	0.85	1.70	800	2	1.96×10^{10}	$(2.6\sim4.0)\times 10^{10}$	1.38@662 keV	1.03
5	USD-W02*	8/14/2018	5-2-17A	1.04	0.34	500	<1	8.18×10^{9}	$(0.5\sim3.0)\times 10^{10}$	2.97@662 keV	1.10
6	USD-R02*	12/13/2018	5-2-17A	0.65	0.39	700	<1	2.93×10^{10}	$(0.5\sim3.0)\times 10^{10}$	2.16@662 keV	1.67
7	USD-R03*	02/27/2019	5-2-17A	0.81	0.54	1400	2	3.78×10^{10}	$(0.5\sim3.0)\times 10^{10}$	2.12@662 keV	1.23
8	USD-RL	05/02/2019	12-20-17A	1.08	3.22	400	7	6.07×10^{9}	$(0.6\sim7.0)\times 10^{10}$	2.55@662 keV	1.93
9	USD-W03*	05/30/2019	5-4-18C	0.94	0.46	1300	<1	2.60×10^{10}	$(1.2\sim2.6)\times 10^{10}$	2.35@662 keV	1.33
10	USD-W04	06/20/2019	12-20-17A	1.08	3.22	300	4	4.55×10^{9}	$(0.6\sim7.0)\times 10^{10}$	2.89@662 keV	2.38
11	USD-W07+	06/23/2020	5-4-18C	0.94	1.96	250	0.4	-	$(1.2\sim2.6)\times 10^{10}$	4.15@662 keV	3.68
12	USD-R04^	03/05/2021	12-20-17A	0.83	1.43	1600	16	4.11×10^{10}	$(0.6\sim7.0)\times 10^{10}$	1.16@60 keV	1.05

*Guard-ring detectors. + Line-contact detector. ^Leakage current measured with the Am-241 source inside the cryostat.

A Summary of Planar Ge Detectors Made at USD

(Cont.)

NO.	Detectors	Fabrication Date	Crystal Number	Thickness (cm)	Active Area (cm^2)	Full Depletion Voltage (V)	Leakage Current @V_d at 79 K (pA)	N_i from C-V Measurements (/cm3)	N_i from Hall effect Measurements (/cm3)	FWHM (keV)	FWHM at Pulser Peak (keV)
13	USD-R08^	04/09/2021	1-24-19A	0.55	1.43	800	20	4.67×10^{10}	$(0.6\sim1)\times 10^{10}$	1.85@60 keV	1.68
14	USD-R09^	04/16/2021	1-24-19A	0.55	1.43	1200	15	4.11×10^{10}	$(0.6\sim1)\times 10^{10}$	1.68@60 keV	1.51
15	USD-R11^	04/23/2021	1-24-19A	0.39	1.43	500	16	7.02×10^{10}	$(0.6\sim1)\times 10^{10}$	2.38@60 keV	2.19
16	USD-R12^	05/19/2021	1-24-19A	0.70	1.43	1300	18	4.70×10^{10}	$(0.6\sim1)\times 10^{10}$	2.32@60 keV	2.17
17	USD-R14	06/25/2021	5-6-21A	0.45	2.56	1600	1	1.40×10^{11}	$(0.7\sim1.8)\times 10^{11}$	1.56@60 keV	1.52
18	USD-W09	02/17/2022	10-23-17C	0.78	0.37	900	0.2	2.62×10^{10}	$(2.6\sim4.0)\times 10^{10}$	1.04@60 keV	0.94
19	USD-KM01	02/25/2022	9-16-21A	0.32	1.44	800	1.7	1.38×10^{11}	$0.3\sim2.0)\times 10^{11}$	1.30@60 keV	1.28
20	USD-W10	03/24/2022	10-23-17C	0.80	0.37	900	0.9	2.50×10^{10}	$(2.6\sim4.0)\times 10^{10}$	0.77@60 keV*	0.75*
21	USD-KM02	03/31/2022	10-23-17C	0.85	0.49	800	0.3	2.21×10^{10}	$(2.6\sim4.0)\times 10^{10}$	0.99@60 keV	0.95

^Leakage current measured with the Am-241 source inside the cryostat.
*The data taking time is not sufficient for measuring the actual FWHM. The actual FWHM should be slightly higher than this value.

A Summary of PPC Ge Detectors Made at USD

NO.	Detectors	Fabrication Date	Crystal Number	Thickness/ Diameter (cm)	PC Diameter (mm)	Full Depletion Voltage (V)	Leakage Current at Full Depletion (pA)	N_i from GeFiCa(/cm^3)	N_i from Hall effect Measurements (/cm^3)	FWHM (keV)	FWHM at Pulser Peak (keV)
1	USD-W06$^+$	02/12/2020	12-20-17A	1.08/N/A	0.6	70	1	3.3×10^9	$(0.6\sim7.0)\times 10^{10}$	3.19 @ 662 keV	1.43
2	USD-K01*	02/21/2020	12-20-17A	0.94/2.34	1.55	170	1.7	-	$(0.6\sim7.0)\times 10^{10}$	2.67 @ 662 keV	1.03
3	USD-R06*	09/04/2020	10-23-17C	0.60	2.5	450	<2	-	$(2.6\sim4.0)\times 10^{10}$	1.10 @ 59.5 keV	0.96

$^+$Planar shape. *Cylindrical shape.

An Example Planar Detector – USD-R03

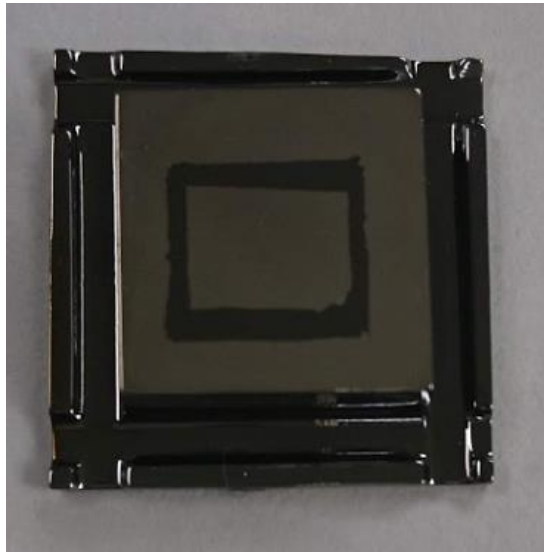

USD-R03

About this detector:

- **Crystal:** USD-5-2-17A
- Detector made by **Rajendra Panth (USD)** using facilities at USD.
- **Dimensions (top):** 1.81 cm (L) × 1.77 cm (W) × 0.81 cm (T)
- **Net impurity concentration**: $3.78 \times 10^{10}/cm^3$
- **Depletion voltage (V_d)**: 1400 V
- **Center contact leakage current at 79 K**: 3 pA @ V_d
- **Mass:** 13.8 g

I-V, C-V and Energy Spectrum Measurements

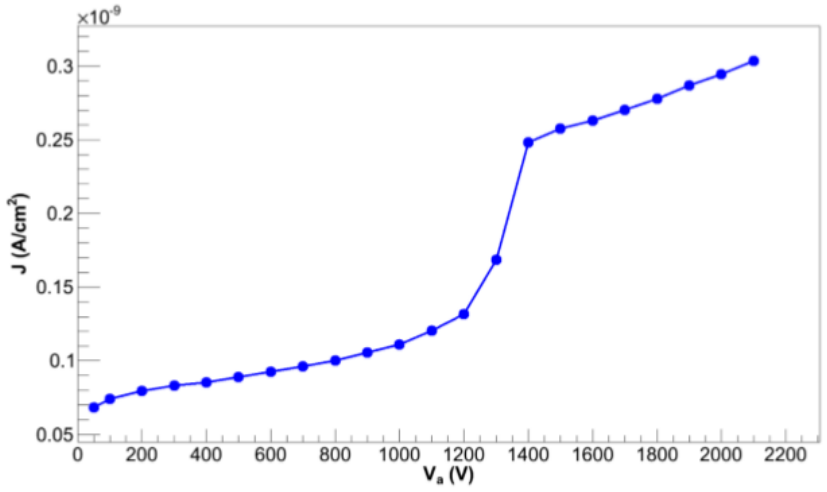

Measured leakage current density plotted as a function of bias voltage at 90 K for detector USD-R03.

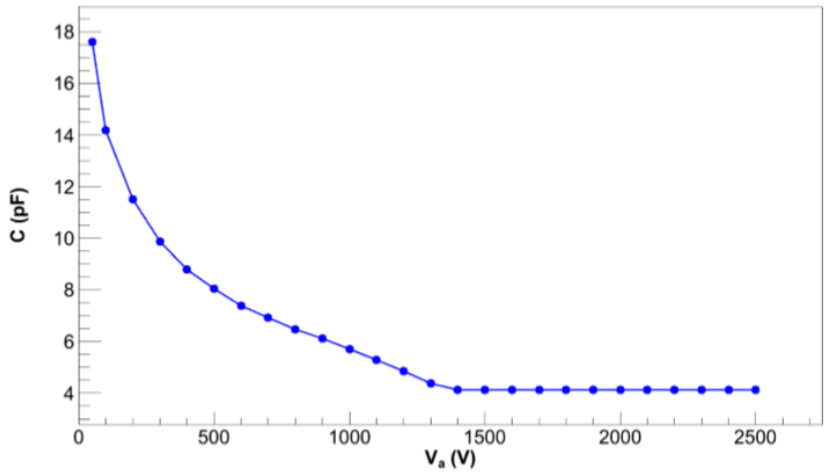

Measured detector capacitance as a function of bias voltage for detector USD-R03 at 79 K.

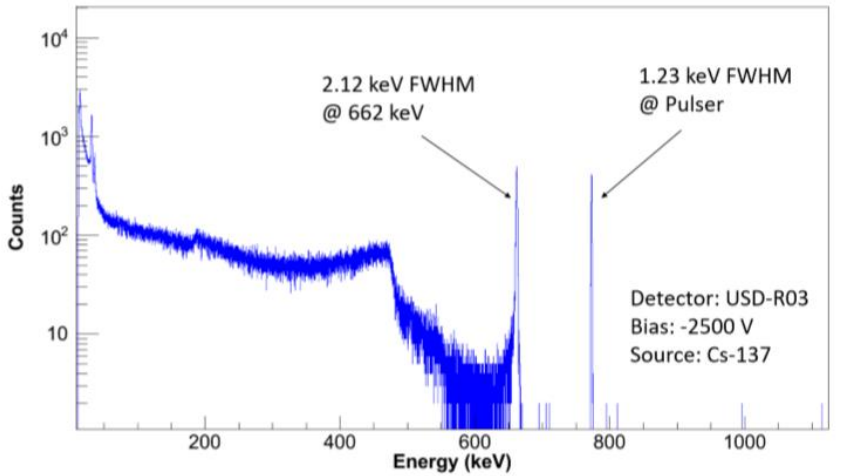

Energy spectrum from a Cs-137 source measured with the detector USD-R03. The source was positioned facing the detector bottom. The bias voltage of -2500 V was applied to the bottom electrical contact on the detector while the signals were measured from the top

Full depletion voltage: $\mathbf{V_{fd} = 1400\ V}$

Crystal impurity concentration: $\mathbf{N = 3.78 \times 10^{10}\ /cm^3}$

A Planar PPC Ge Detector with a-Ge Contact Made at USD

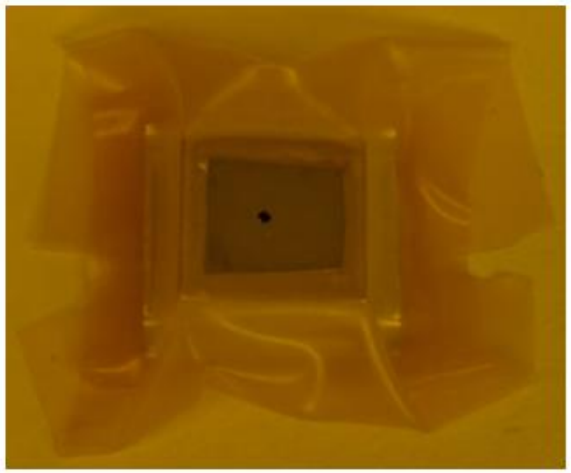

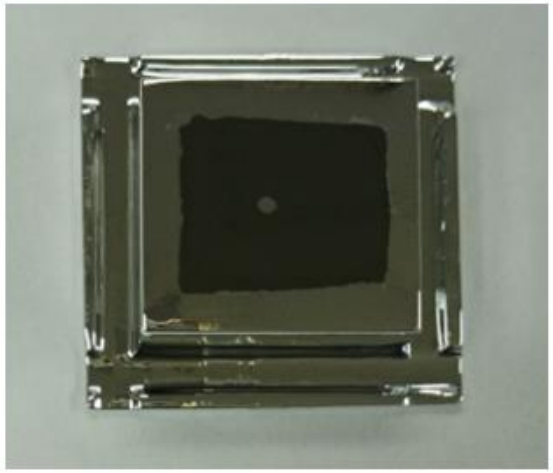

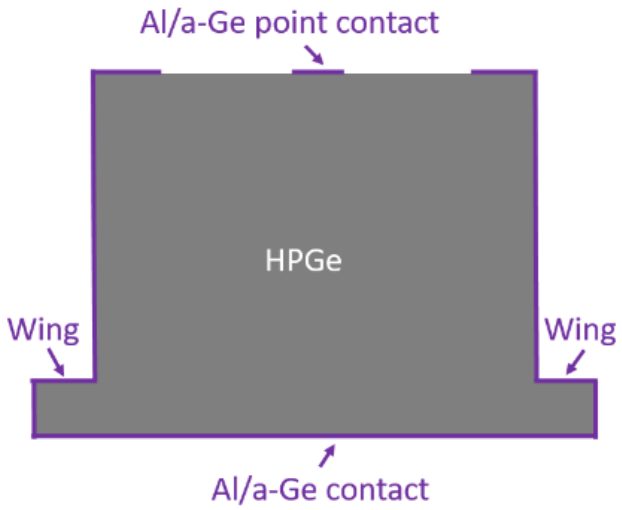

About this detector (USD-W06):

- **Crystal:** USD-12-20-17A
- Detector made by **Wenzhao Wei (USD)** using facilities at USD.
- **Impurity Concentration:** $3.3\times10^{9}/cm^{3}$
- **Depletion voltage (V_d):** 60 V
- **Leakage current:** 0.5 pA @ V_d
- **Thickness:** 0.94 cm
- **Bottom Length and Width:** 2.12 cm and 2.08 cm
- **Top (outer) Length and Width:** 1.37 cm and 1.37 cm
- **Top (inner) Length and Width:** 0.77 cm and 0.77 cm
- **PC Diameter:** ~0.6 mm
- **Mass:** 9.7 g

Detector Performance at 79 K

Shown is the detector USD-W06 loaded in a variable temperature cryostat for characterization.

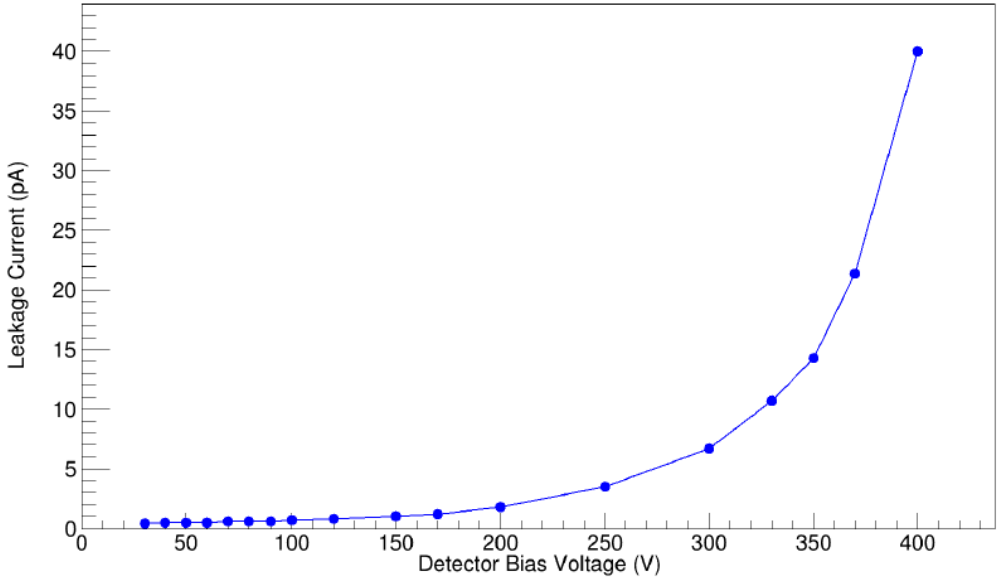

Measured leakage current as a function of bias voltage at 79 K for detector USD-W06.

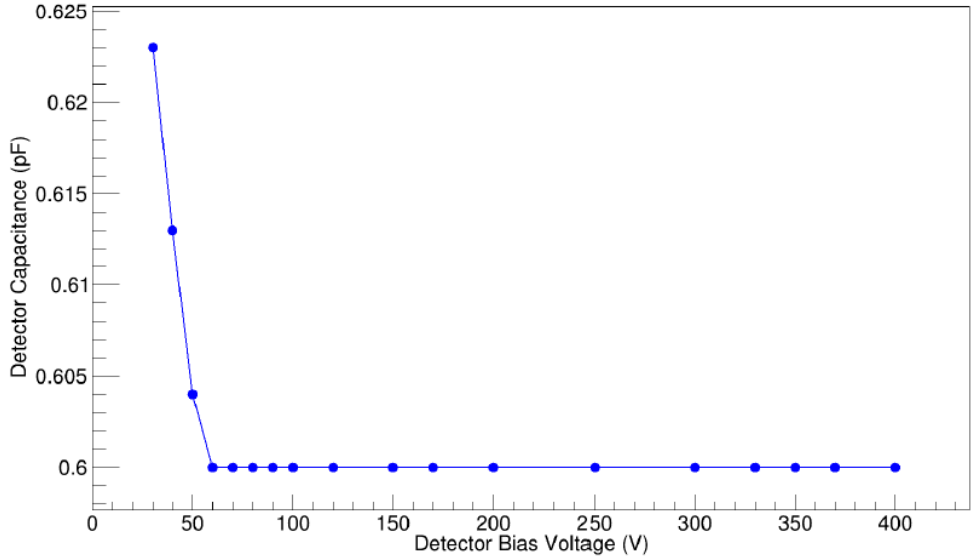

Measured detector capacitance as a function of bias voltage at 79 K for detector USD-W06.

Detector Performance at 79 K (Cont.)

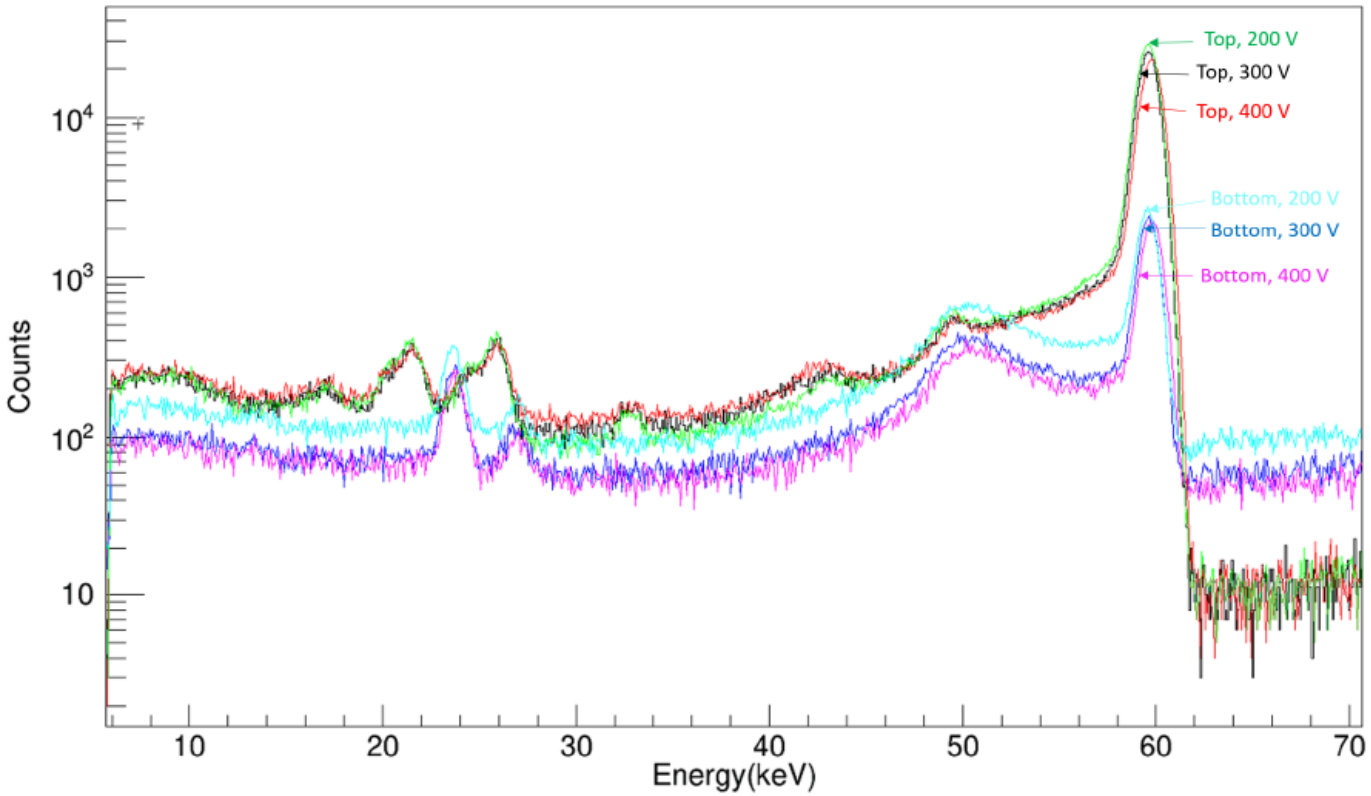

Energy spectra of a Am-241 source measured with the detector USD-W06. The spectra were taking at three voltages, 200 V, 300 V and 400 V with the source placed at the top and the bottom of the cryostat, respectively.

Energy Peak (keV)	FWHM at the energy peak (keV)	FWHM at the pulser (keV)	Relative statistic driven energy resolution (%)
24	1.11	1.06	1.37
27.5	1.17	1.06	1.80
59.5	1.16	1.06	0.79

The FWHM of three energy peaks from Am-241 and the pulser peak at 400 V when the source was placed at the bottom of the cryostat. The energies presented here are the expected values. For each energy peak, the relative statistic driven energy resolution was determined by subtracting in quadrature the FWHM at the pulser from the FWHM at the energy peak and then divided by the energy.

*This study has been converted into a scientific paper. For more information, please refer to EPJ C **82**, 203 (2022), or arXiv: 2105.02109.*

Cylindrical Mini-PPC with Li/Al and a-Ge/Al Contacts

Lithiation

Sputtering

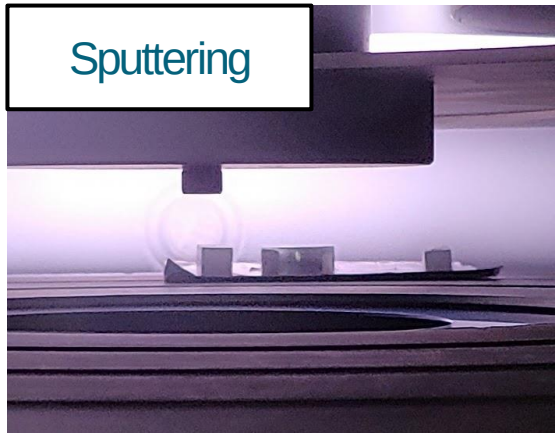

Contact Formation

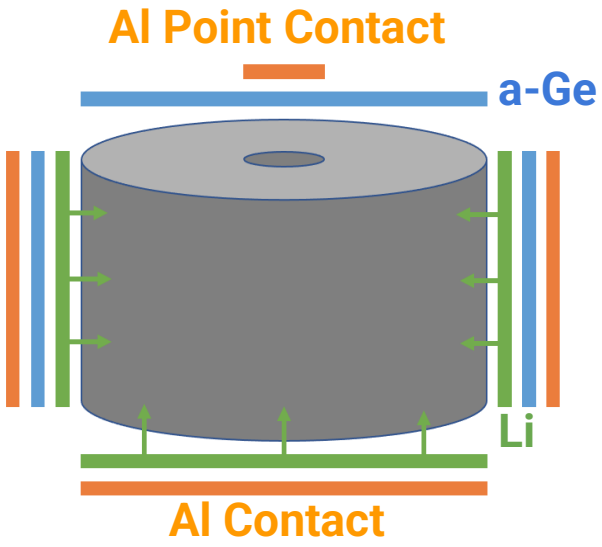

About this detector (USD-K01):

- **Crystal:** USD-12-20-17A
- Detector made by **Kyler Kooi (USD)** using facilities at Lawrence-Berkeley Lab and USD.
  - **LBL:** Mechanical processing and Lithiation
  - **USD:** a-Ge, Al sputtering, Testing
- **Impurity Concentration:** $(4\sim5)\times10^{9}/cm^{3}$
- **Depletion Voltage:** 170 V
- **Leakage Current:** <1.5 pA up to 1000 V
- **Height:** 9.4 mm
- **Diameter:** 23.4 mm
- **PC Diameter:** 3.1 mm
- **PC Height:** 0.4 mm
- **Mass:** 21.5 g

Detector Performance at 79 K

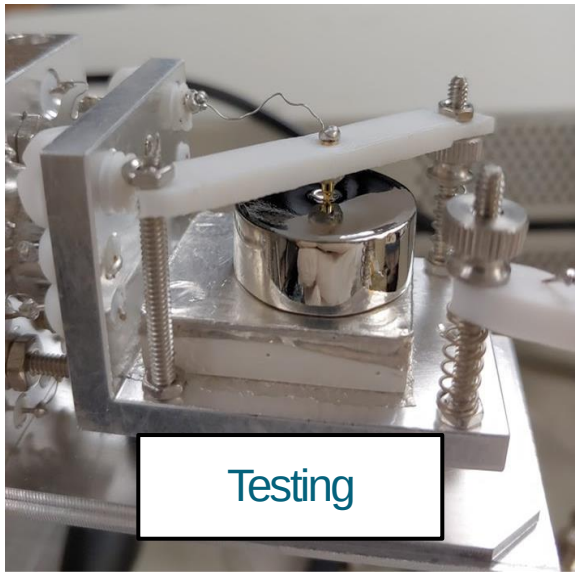

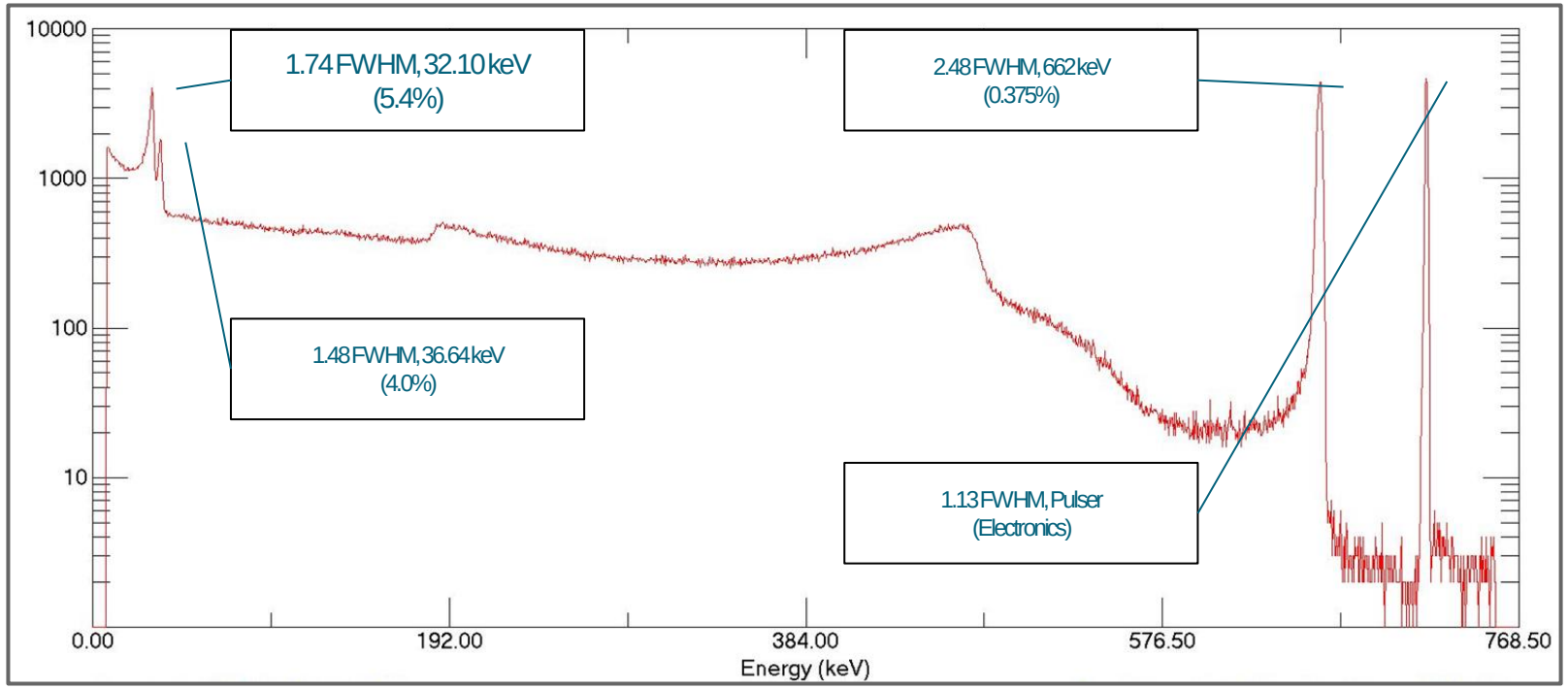

Cs-137 Energy Spectrum (650 V, 100 minutes)

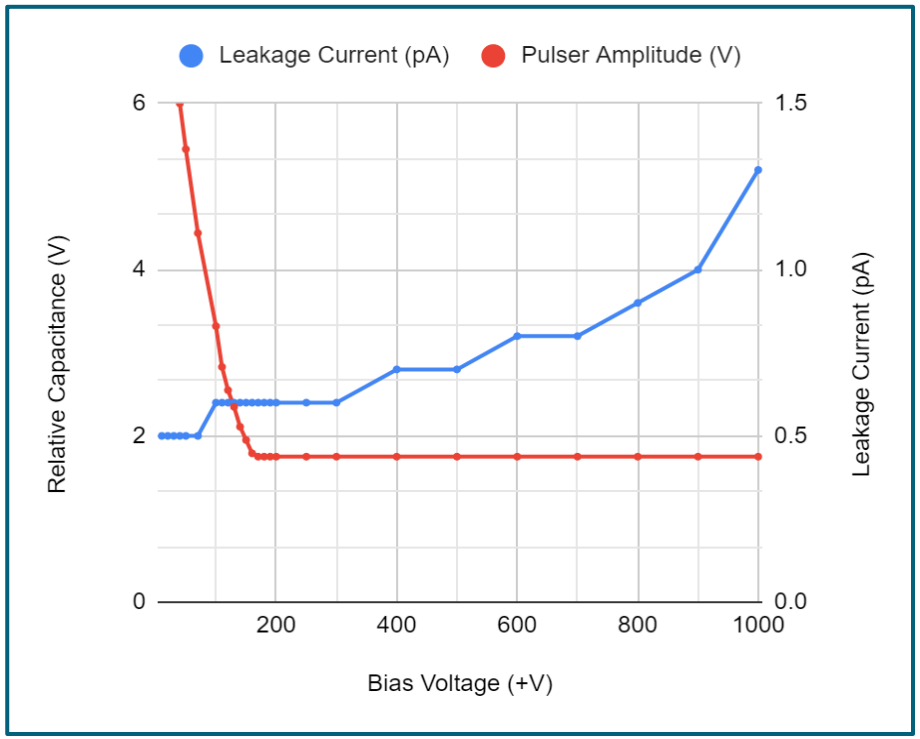

A Cylindrical PPC Ge Detector with a-Ge Contact Made at USD

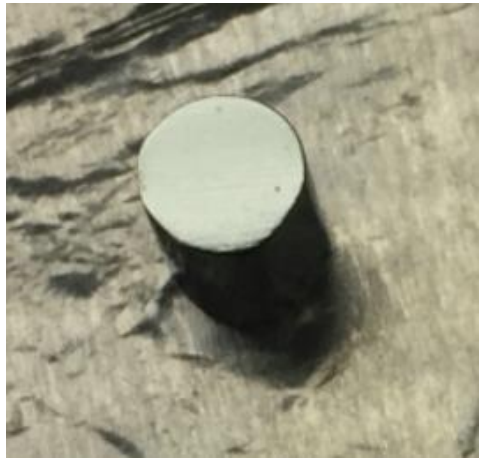

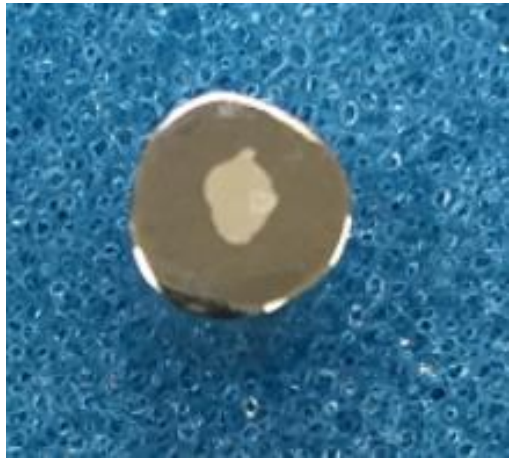

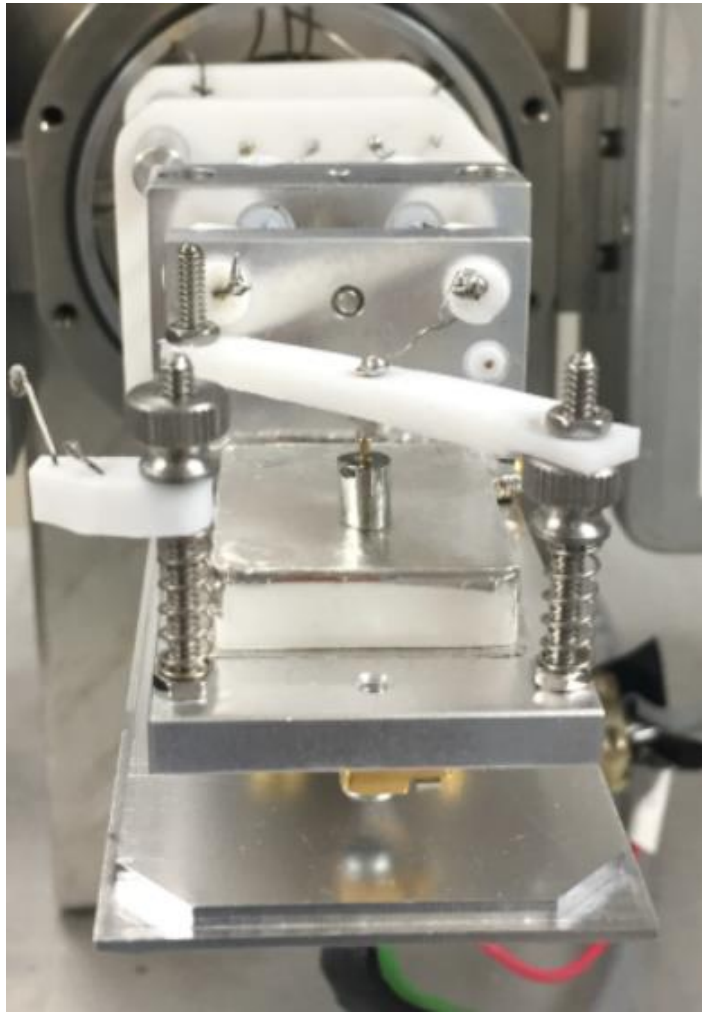

About this detector (USD-R06):

- Crystal: USD-10-23-17C
- This crystal was cut by Prof. Rusty Harris' group at TAMU.
- The detector was made by **Rajendra Panth (USD)** at USD.
- Height: 6.0 mm
- Diameter: 5.5 mm
- Point contact diameter: ~2.5 mm
- Depletion voltage: 450 V
- Leakage current at depletion voltage: <2 pA

Detector Performance at 79 K

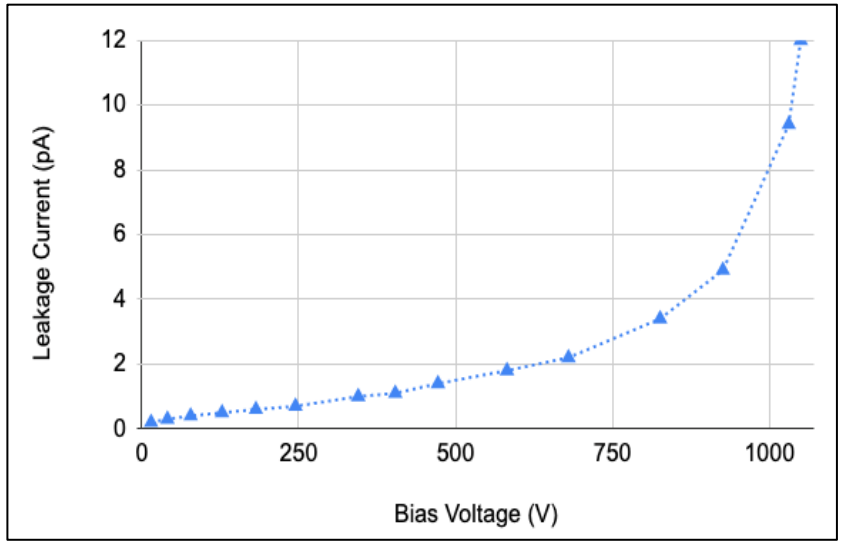

Measured leakage current as a function of bias voltage at 79 K.

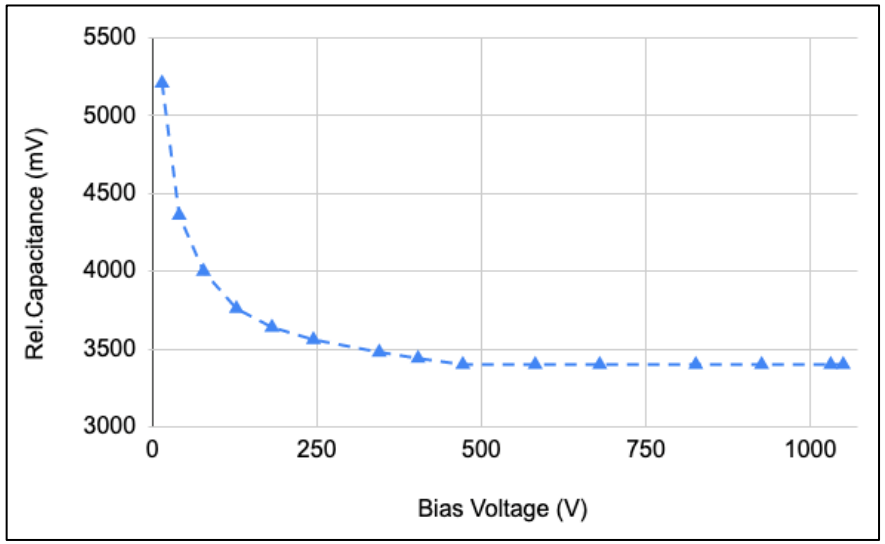

Measured relative detector capacitance versus bias voltage at 79 K.

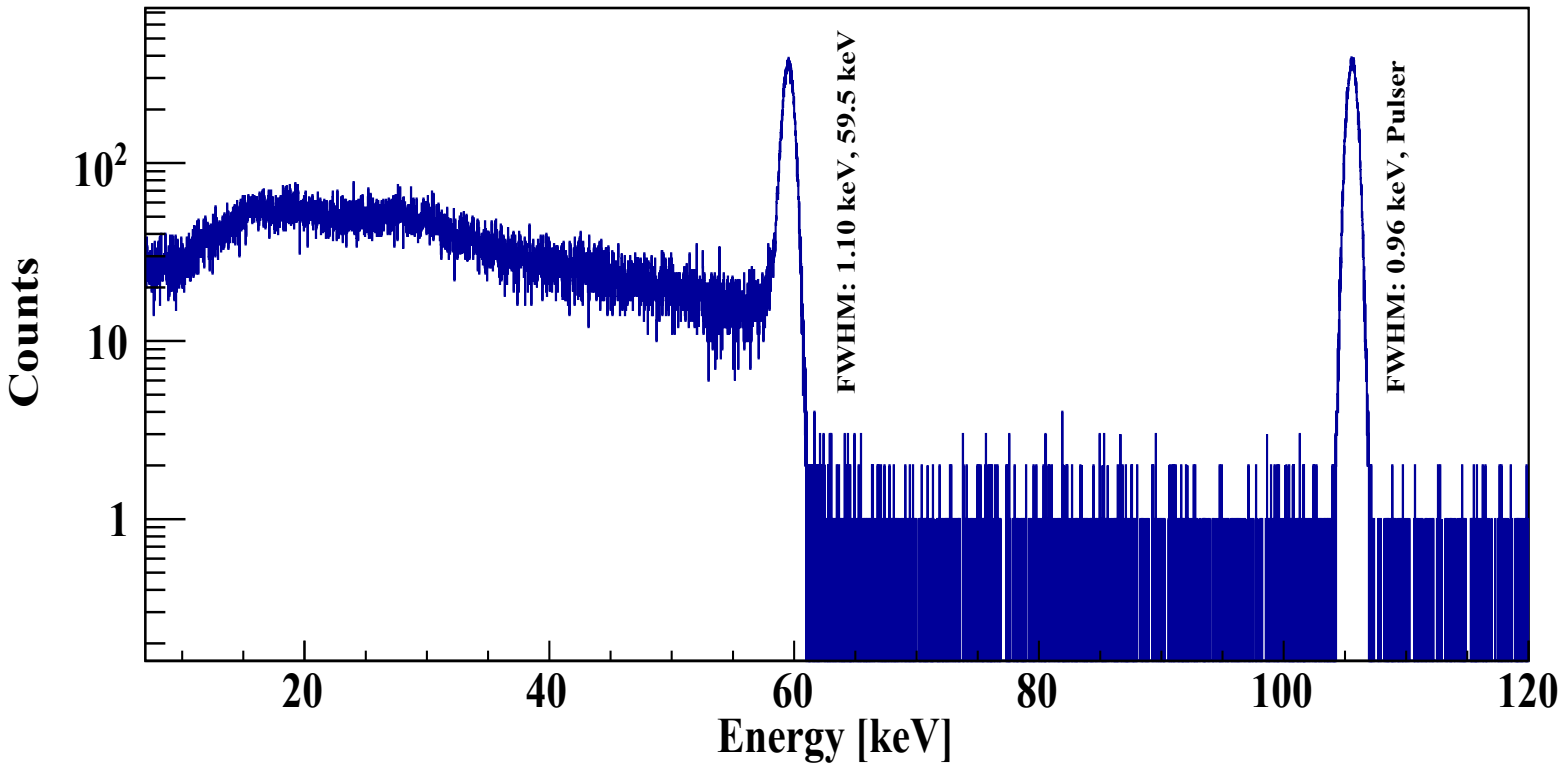

Energy spectrum from an Am-241 source measured with the detector. The source was positioned facing the detector top. A bias voltage of-1050 V was applied to the bottom of the detector while the signals were read-out from the top.

R&D of Ge Ring-Contact Detectors at USD

(Funded by NSF)

R&D of Ge Ring-Contact (GeRC) Detectors

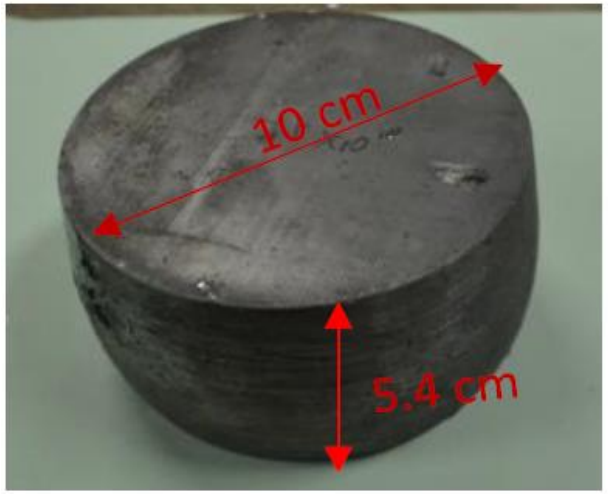

A USD-grown crystal with a mass of 2.2 kg and an impurity concentration of (2.06 ~ 2.68) × 10^{10}/cm^3 from Hall effect system.

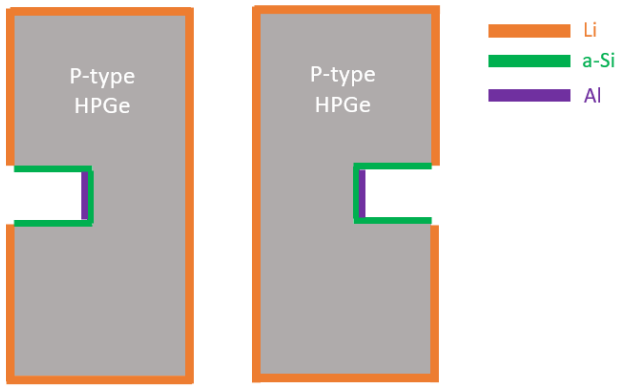

Schematic cross-sectional drawing of the detector geometry.

(suggested by Dr. David Radford from ORNL)

- **Project Goal:** To advance novel Ge detector technology – GeRC in order to study the flexibility of using large-size Ge detectors for LEGEND-1000. To achieve this goal, the following three objectives are determined:

1. Fabricate the first GeRC detector with a mass of ~2 kg from an existing USD-grown crystal. The fabrication will be conducted in Prof. Rusty Harris's lab at TAMU.
2. If the detector is successful, we will investigate the energy resolution and pulse shape properties of this detector. The characterization will be conducted in Prof. John Wilkerson's lab at UNC.
3. Grow a new crystal with a mass of >3 kg for fabrication and characterization of the second GeRC detector.

Two Crystals for Test Fabrication

- **Crystal**: 7-13-16A
- **Mass**: 627 g
- **Diameter**: 68 mm
- **Thickness**: 30 mm
- **Impurity Level:**
  Top: 6.7× $10^{10}/cm^3$
  Bottom: 1.0× $10^{10}/cm^3$

Crystal #1

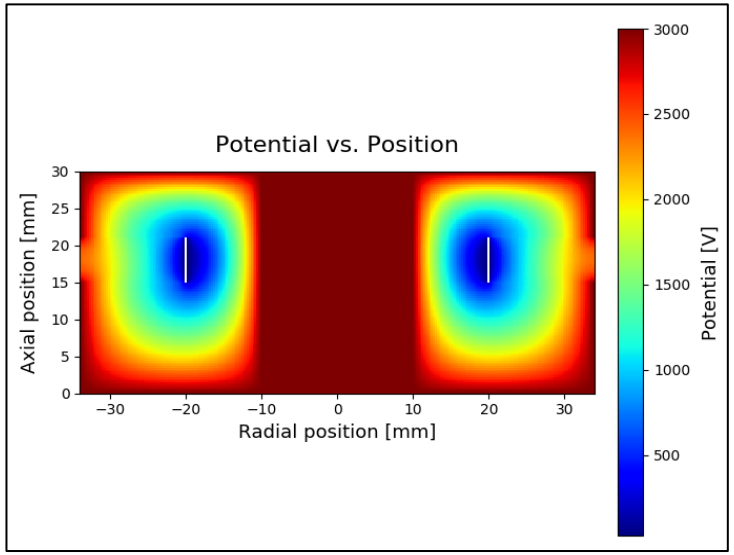

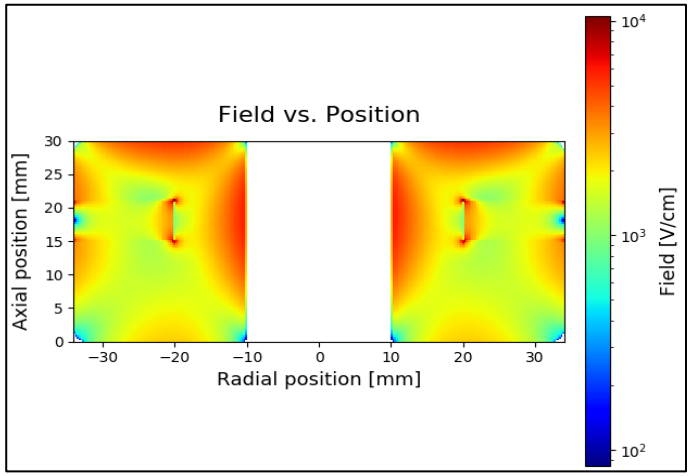


```
>>  Calculated capacitance at 3000 V: 31.219 pF
Writing weighting potential to file fields/wp_usd1.dat
Estimated depletion voltage (or pinch-off?) = 2271 V
Minimum bulk field = 1062.0 V/cm at (r,z) = (23.2, 21.5) mm
```

- **Crystal**: 12-18-19A
- **Mass**: 384 g
- **Diameter**:
  Top: 65 mm
  Bottom: 72 mm
- **Thickness**:
  Left: 21 mm
  Right: 18 mm
- **Impurity Level:**
  Top: (2.4~2.7)× $10^{10}/cm^3$
  Bottom: 1.6× $10^{10}/cm^3$

Crystal #2 (backup)

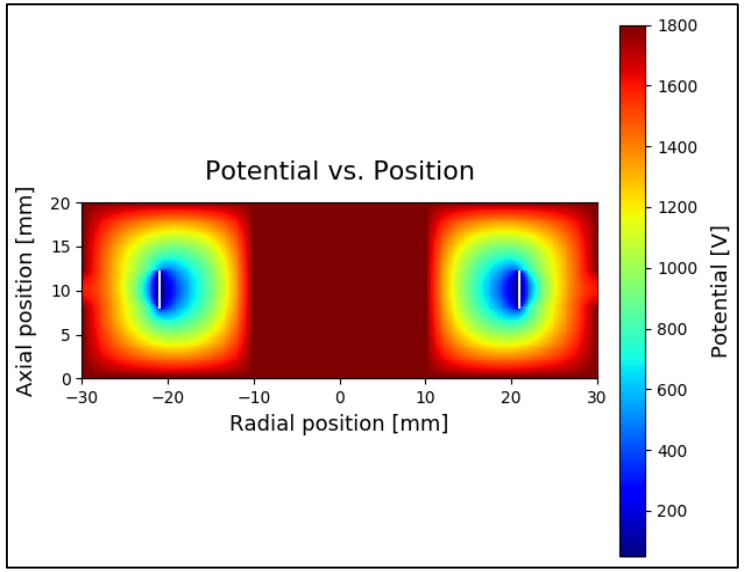

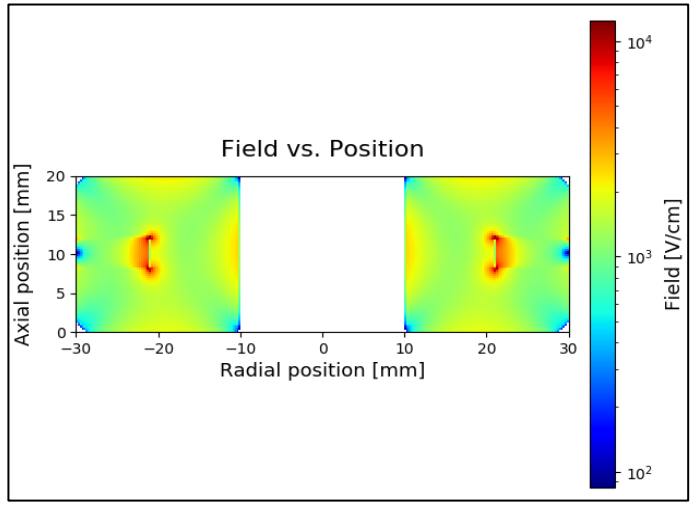


```
>>  Calculated capacitance at 3000 V: 31.219 pF
Writing weighting potential to file fields/wp_usd1.dat
Estimated depletion voltage (or pinch-off?) = 2271 V
Minimum bulk field = 1062.0 V/cm at (r,z) = (23.2, 21.5) mm
```

About USD Crystal 10-23-17C

- Mass: 2247g
- Diameter: 10cm
- Thickness: 5.4cm
- Impurity Level: $2.06 \times 10^{10}(top) \sim 2.68 \times 10^{10}/cm^3\,(bottom)$

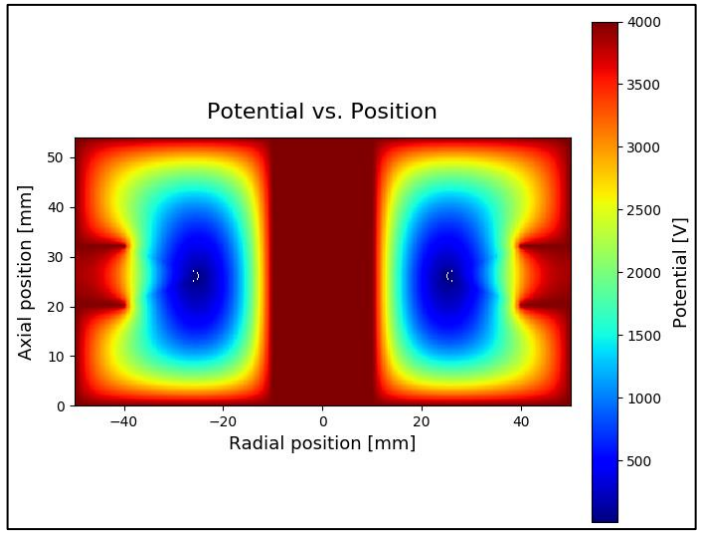

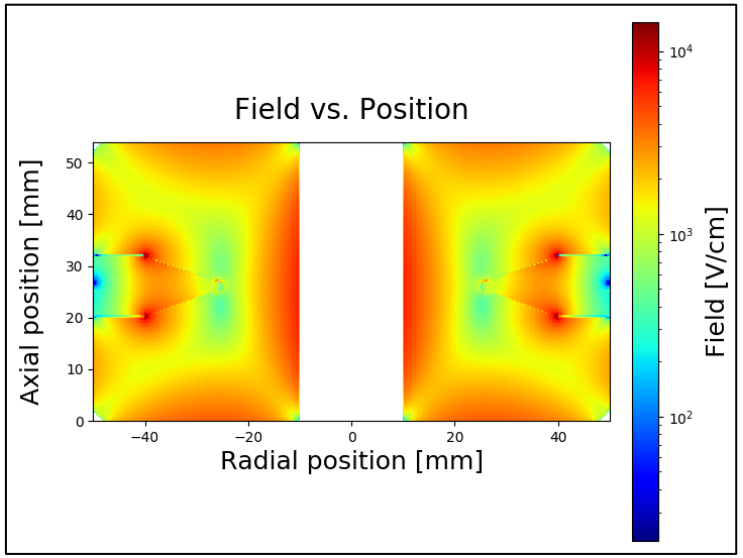

Detectors	Impurity from C-V Measurements
USD-L06	$2.94\times10^{10}/cm^3$
USD-L07	$2.45\times10^{10}/cm^3$
USD-L08	$1.96\times10^{10}/cm^3$
USD-W09[+]	$2.62\times10^{10}/cm^3$
USD-W10	$2.50\times10^{10}/cm^3$
USD-KM02	$2.21\times10^{10}/cm^3$

[+] W09 is made from L07.

Input:

1. Impurity concentration: (2.06 ~2.94) $\times10^{10}/cm^3$
2. Applied bias voltage: 4000 V on the n+ contact.
3. The same height and radius as the real crystal.
4. Hole diameter: 20 mm

Output from Siggen:

```
>>  Calculated capacitance at 4000 V: 28.639 pF
Writing weighting potential to file fields/wp_usd.dat
Estimated depletion voltage (or pinch-off?) = 3729 V
Minimum bulk field = 356.9 V/cm at (r,z) = (25.5, 25.0) mm
```

R&D of Thin-Contact ICPC Ge Detectors (Under Plan)

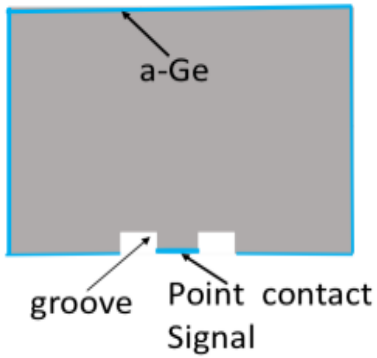

Fig. 1: A sketch of a BEGe detector geometry.

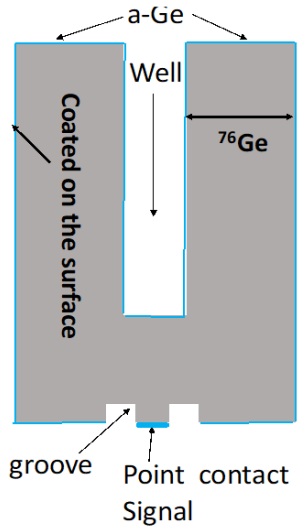

Fig. 2: A sketch of a thin-contact ICPC detector geometry.

- **Project Goal:**
  - Advance the novel Ge detector technology, ICPC, with thin contact made of a-Ge (~600 nm) in order to study an alternative technology option in background rejection for LEGEND.

- **Project objectives:**
  1. Measurements of the dead layer of thin-contact detectors using the existing mini-PPC detectors with ^{90}Sr and ^{241}Am sources to study the surface events response and their pulse shape properties.
  2. Proof of the thin-contact technology with an existing USD-grown crystal by fabricating a thin-contact broad energy Ge (BEGe) detector (Fig. 1).
  3. Growth of large-size crystals to fabricate a thin-contact ICPC detector (Fig. 2) with a mass of >2 kg for studying the energy resolution, the pulse shape properties, and the long-term stability by deploying the detector in LAr. We will focus on testing its robustness in handling using glovebox.
  4. R&D of sputtering a thin film (~1mm) of PEN (polyethylene naphthalate) onto the outer surface layer of the thin-contact detectors to reduce the surface α and β particles from ^{210}Pb and ^{42}K decays.

Modularized HPGe Detector System for Undergraduate Education

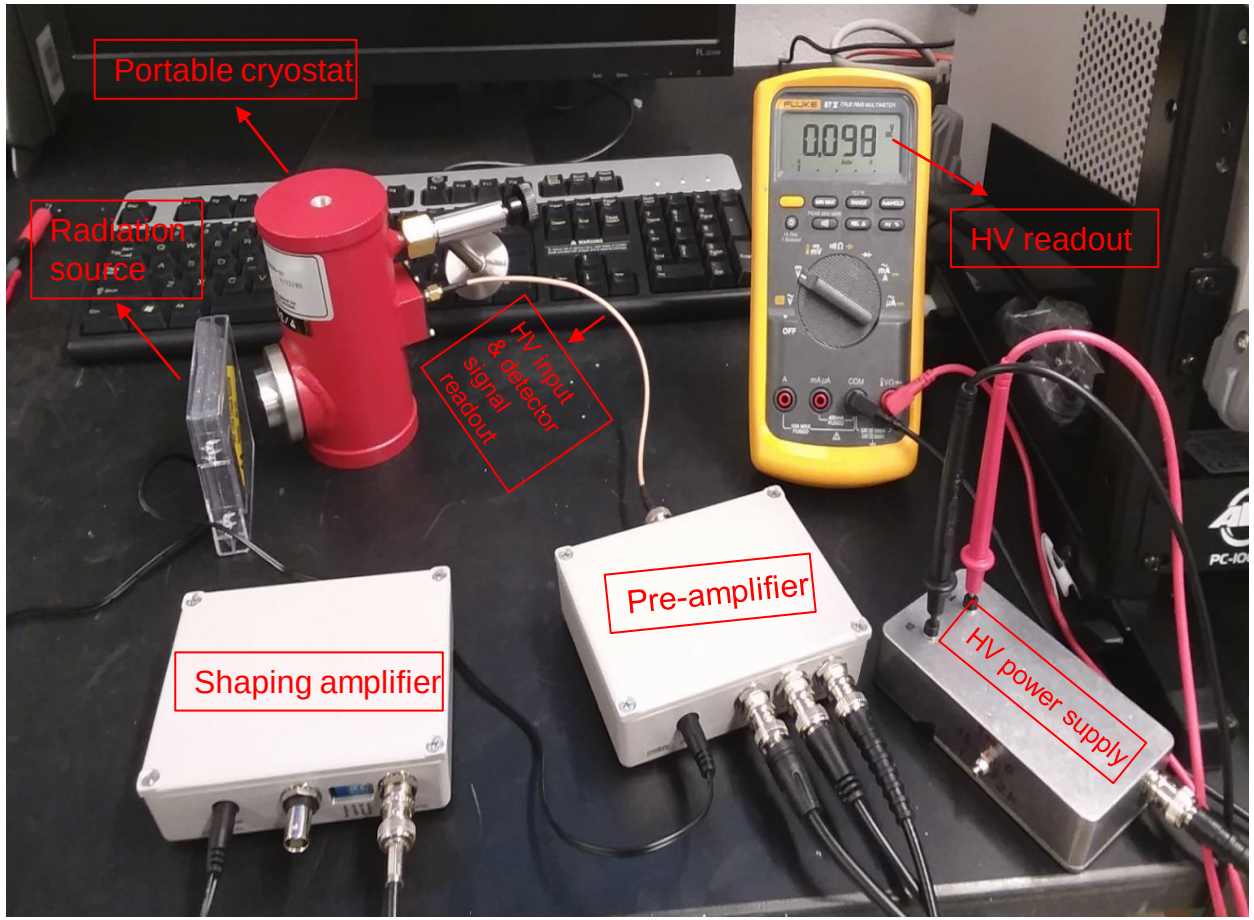

Modularized HPGe detector system.

- **Project leader:** Prof. Jing Liu at USD
- **Project goal:** Develop an affordable and easy-to-access Ge detector testing system for undergraduate students to learn about Ge detectors.

Inside view of the portable cryostat.

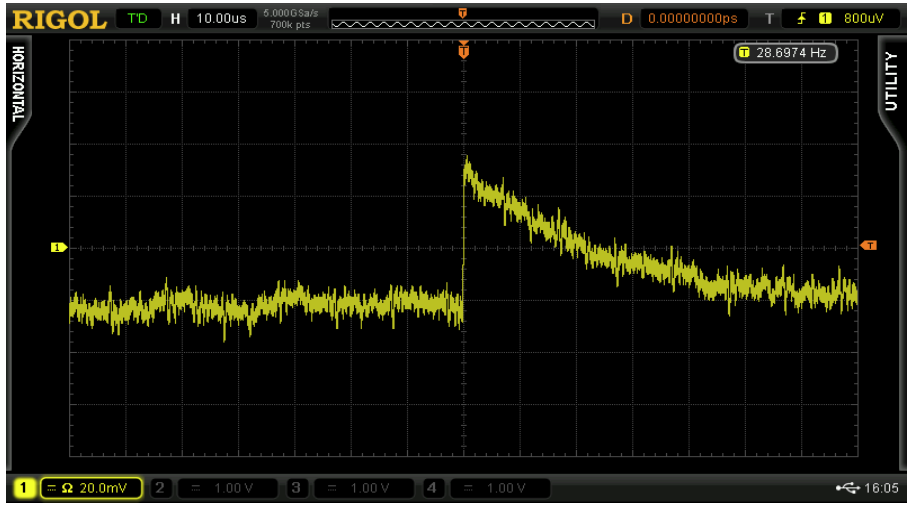

A typical signal pulse.
(we are working on reducing the electronic noise to improve the performance.)

Conclusions

- USD Ge detector group has successfully fabricated 21 small planar detectors and 3 mini-PPC detectors with good detector performance so far using USD-grown crystals.
- Three new types of Ge detectors including GeICA, GeRA and thin-contact ICPC are under development at USD for low-mass dark matter and $0\nu\beta\beta$ decay searches.
- A modularized HPGe detector testing system is under development at USD for undergraduate students to learn about Ge detectors.
- USD is able to characterize Ge detectors at both 79 K and 4 K.
- A new sputtering system funded by NSF is expected to be installed at USD this summer. This will allow us to fabricate large-size Ge detectors in the future.

References

[1] M. Amman, P.N. Luke, S.E. Boggs, Amorphous-semiconductor-contact germanium-based detectors for gamma-ray imaging and spectroscopy, *NIM* A **579** (2007) 886-890.

[2] I. Alkhatib et al. (SuperCDMS Collaboration), Light Dark Matter Search with a High-Resolution Athermal Phonon Detector Operated above Ground, *Phys. Rev. Lett.* **127**, 061801 (2021).

[3] N. Abgrall et al. (LEGEND Collaboration), LEGEND-1000 Preconceptual Design Report, arXiv: 2107.11462v1.

[4] Martin Hoferichter, Javier Menéndez, Achim Schwenk, Coherent elastic neutrino-nucleus scattering: EFT analysis and nuclear responses, *Phys. Rev. D* **102**, 074018 (2020).

[5] H.T. Wong, *Mod. Phys. Lett. A* **23**, 1431 (2008); S.T. Lin et al., *Phys. Rev. D* **79**, 061101(R) (2009).

[6] Refer to MJD website: https://www.npl.washington.edu/majorana/design-technologies.

[7] M. Agostini et al. (GERDA Collaboration), Characterization of 30 ^{76}Ge enriched Broad Energy Ge detectors for GERDA Phase II, *Eur. Phys. J. C* **79** (2019) 978.

[8] D.-M. Mei et al. Direct detection of MeV-scale dark matter utilizing germanium internal amplification for the charge created by the ionization of impurities, *EPJ C* **78** (2018) 187.

[9] Jianchen Li, Jing Liu and Kyler Kooi, HPGe detector field calculation methods demonstrated with an educational program, GeFiCa, *Eur. Phys. J. C* **80**, 230 (2020).

Thanks!

Backup Slides

About Internal Charge Amplification

- The detection of low-energy deposition in the range of sub-eV through ionization using germanium (Ge) with a bandgap of ~ 0.7 eV requires internal amplification of the charge signal. This can be achieved through high electric field that accelerates charge carriers, which can then generate more charge carriers.

- With large localized E-fields, the ionized excitations can be accelerated to kinetic energies larger than the Ge bandgap at which point they can create additional electron–hole pairs, producing intrinsic amplification to achieve an ultra-low energy threshold of ~ 0.1 eV for detecting low-mass DM particles in the MeV scale.

- In comparison with the current SuperCDMS and EDELWEISS experiments, there are two main differences: (1) **charge creation** and (2) **internal amplification**. For the former, *in our technology, the charge is created by ionization of impurities*, which allows an experiment to access even lower energy deposition (~ 0.1 eV) comparing to SuperCDMS or EDELWEISS at which the charge is mostly created by ionization of Ge (~ 50 eV). In the case of the latter, we propose to internally amplify charge using *avalanche* while SuperCDMS and EDELWEISS internally amplify signal through emission of Luke phonons.

Please refer to our paper, EPJ C 78, 187 (2018) for more information.

About Sputtering

Process of Sputtering

The principle of Sputtering is to use the energy of a plasma (partially ionized gas) on the surface of a target (cathode), to pull the atoms of the material one by one and deposit them on the substrate.

To do this, a plasma is created by ionization of a pure gas (usually Argon) by means of a potential difference (pulsed DC), or electromagnetic excitation (MF, RF); this plasma is composed of Ar^+ ions which are accelerated and confined around the target due to the presence of a magnetic field. Each ionized atom, by striking the target, transfers its energy and rips an atom, having enough energy to be projected to the substrate.

The plasma is created at relatively high pressures (10^{-1} - 10^{-3} mbar), but it is necessary to start from a lower pressure before the introduction of Argon, to avoid contamination due to the residual gases.

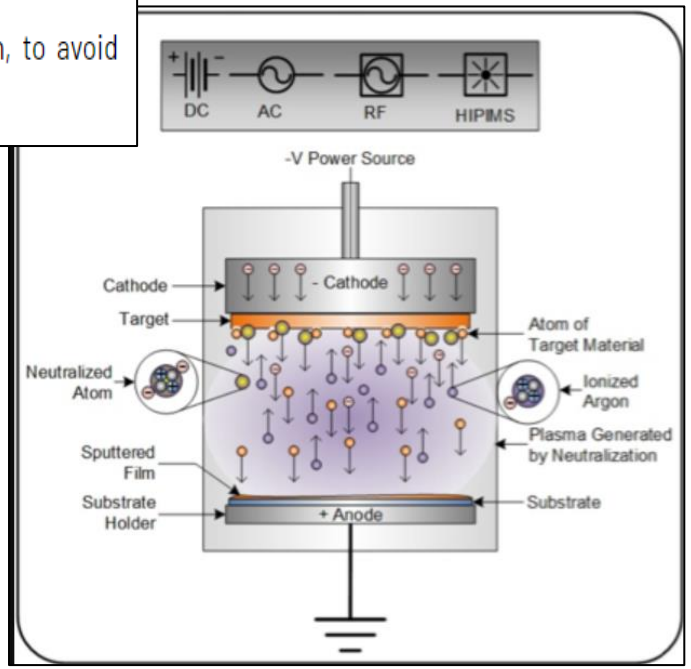

About Sputtering

Benefits

1. Insulators (e.g. aluminum oxide or boron nitride) and semiconductors can also be sputtered

2. the substrate heats up less

Types of Sputtering

The main types of Sputtering are discussed below:

1. DC diode sputtering

With a DC voltage = 500 - 1000 V, an argon low-pressure plasma is ignited between a target and a substrate. Positive argon ions precipitate atoms out of the target, which then migrates to the substrate and condenses there.

Limitations

Only electrical conductors can be sputtered, as otherwise an opposing field builds up and the sputtering process stops. The other limitation is that only low sputtering rates are achieved since only a few argon ions are formed.

2. RF sputtering

In radio frequency sputtering, a high-frequency alternating field is applied instead of the DC electric field. The necessary high-frequency voltage source is connected in series with a capacitor and the plasma. The capacitor serves to separate the DC component and to keep the plasma electrically neutral.

The alternating field accelerates the ions and the electrons alternately in both directions. From a frequency of approximately 50 kHz, the ions can no longer follow the alternating field due to their much smaller charge-to-mass ratio.

The electrons oscillate in the area of the plasma and there are more and more collisions with argon atoms. This results in a high plasma rate, a consequence of which is the possible pressure reduction to about 10^{-1} - 10^{-2} Pa) with the same sputtering rate. This allows the production of thin layers with a different microstructure than would be possible at higher pressures.

The positive ions move through a superimposed negative offset voltage on the target in the direction of the target and solve as in DC sputtering by collision atoms from the target material. The subsequent sputter deposition corresponds to that of other sputtering methods.

Fig. 7

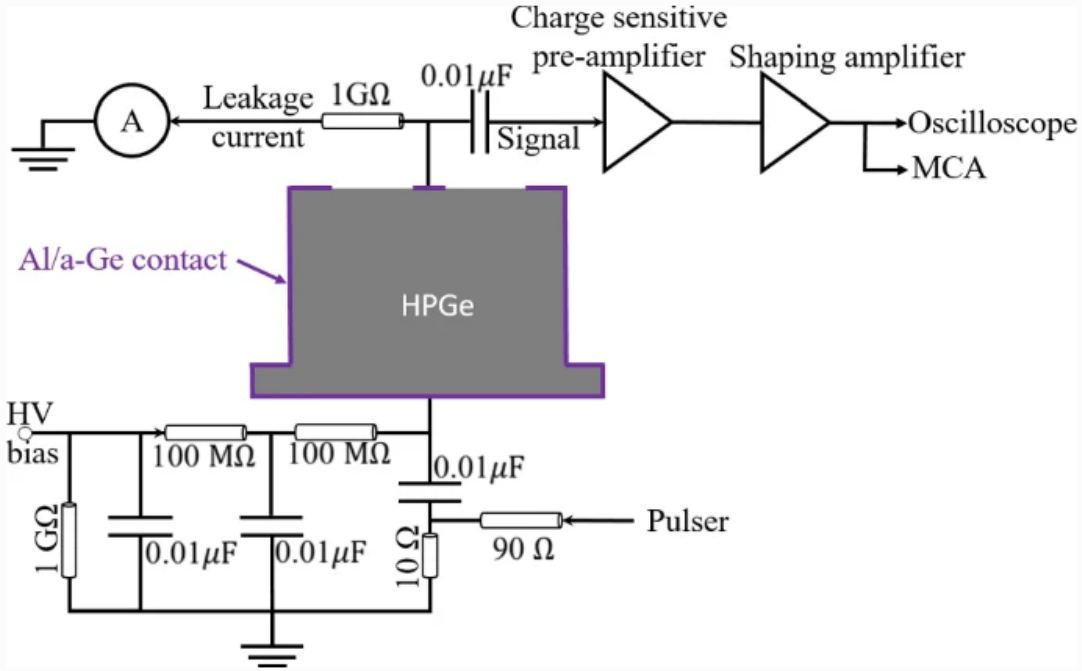

Electronic circuit for detector characterization

*W.-Z. Wei et al. EPJ C **82**, 203 (2022)*

3.2 *C-V* Characteristics

The main purpose of the *C-V* measurements (i.e. detector capacitance as a function of the detector bias voltage) is to determine the full depletion voltage of the detector and in turn the impurity concentration of the crystal. This can be done by applying a small voltage step from the pulser plus a constant voltage from the high voltage (HV) power supply, as shown in the diagram in figure 4. The capacitance (C) of a planar Ge detector is similar to that of two flat, parallel metallic plates. That is:

$$C = \frac{\varepsilon_0 \varepsilon_{Ge} A}{t_d}, \tag{3.5}$$

where A is the active cross-section area of the detector and t_d is the depletion depth of the detector, which is related to the applied detector voltage (V) through:

$$t_d = \left(\frac{2\varepsilon_0 \varepsilon_{Ge} V}{qN}\right)^{1/2}, \tag{3.6}$$

where q is the elementary charge and N is the impurity concentration of the crystal.

*W.-Z. Wei et al. JINST **13** (12), P12026 (2018)*

A Summary of Published Papers on Ge Detectors Made at USD

1. W.-Z. Wei, H. Mei, K. Kooi, D.-M. Mei, J. Liu, J.-C. Li, R. Panth, and G.-J. Wang, Development of Planar P-type Point Contact Germanium Detectors for Low-Mass Dark Matter Searches, submitted to *The European Physical Journal C 82, 203 (2022).*
2. R. Panth, W.-Z. Wei, D.-M. Mei, J. Liu, S. Bhattarai, H. Mei, M. Raut, P. Acharya, K. Kooi, and G.-J. Wang, Implication of the Temperature-Dependent Charge Barrier Height of Amorphous Germanium Contact Detector in Searching for Rare Event Physics,, arXiv: 2101.09322 (2021).
3. W.-Z. Wei, R. Panth, J. Liu, D.-M. Mei. H. Mei and G.-J. Wang, The Impact of the Charge Barrier Height on Germanium (Ge) Detectors with Amorphous-Ge Contacts for Light Dark Matter Searches, *The European Physical Journal C* **80,** 472 (2020).
4. R. Panth, J. Liu, I. Abt, X. Liu, O. Schulz, W.-Z. Wei, H. Mei, D. -M. Mei and G.-J. Wang, Characterization of high-purity germanium detectors with amorphous germanium contacts in cryogenic liquids, *The European Physical Journal C* **80,** 667 (2020).
5. S. Bhattarai, R. Panth, W.-Z. Wei, H. Mei, D.-M. Mei, M.S. Raut, P. Acharya and G.-J. Wang, Investigation of the Electrical Conduction Mechanisms in P-type Amorphous Germanium (a-Ge) Used as a-Ge Contacts for Ge Detectors, *The European Physical Journal C* **80,** 950 (2020).
6. M. Raut, H. Mei, D.-M. Mei , S. Bhattarai, W.-Z. Wei, R. Panth, P. Acharya and G.-J. Wang, Characterization of High-Purity Germanium (Ge) Crystals for Developing Novel Ge Detectors, *Journal of Instrumentation* **15** (2020) T10010.
7. X.-H. Meng, G.-J. Wang, M.-D. Wagner, H. Mei, W.-Z. Wei, J. Liu, G. Yang and D.-M. Mei, Fabrication and Characterization of High-Purity Germanium Detectors with Amorphous Germanium Contacts, *Journal of Instrumentation* **14** (2019) P02019.
8. W.-Z. Wei, X.-H. Meng, Y.-Y. Li, J. Liu, G.-J. Wang, H. Mei, G. Yang, D.-M. Mei and C. Zhang, Investigation of Amorphous Germanium Contact Properties with Planar Detectors Made from USD-Grown Germanium Crystals, *Journal of Instrumentation* **13** (2018) P12026.

Comparison between Monte Carlo and Data

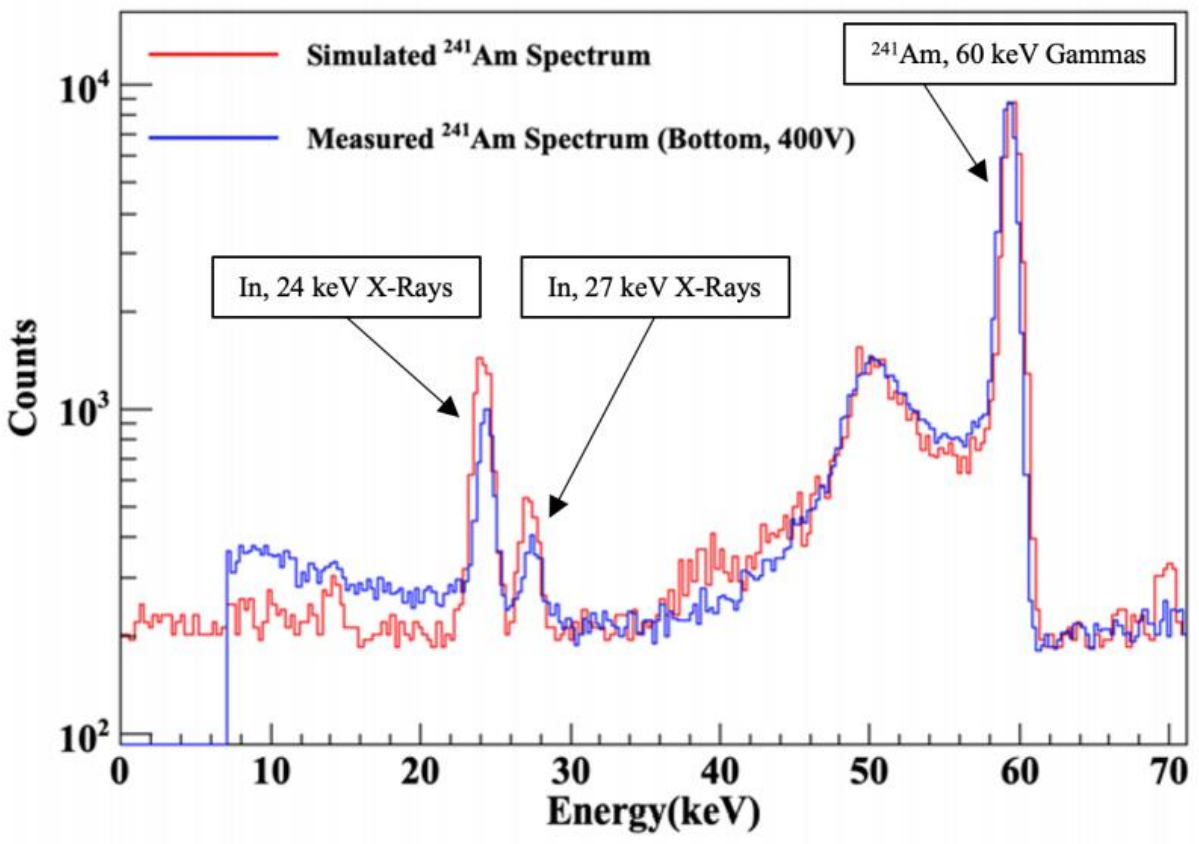

A comparison between the Monte Carlo simulation and the measurement when the source was placed at the bottom.

- We conducted a Geant4-based Monte Carlo simulation for the source at the bottom with a detailed geometry of the cryostat.
- The comparison between simulation and data confirmed that the two distinct X-rays (24 keV and 27.5 keV) observed in the data are from indium due to the process of fluorescence when 59.5 keV gamma ray interacted with the indium foil which is close to the detector on the inside of the cryostat.
- These two distinct X-rays provide a good opportunity to exam the detector energy resolution for low-energy X-rays with energy below 59.5 keV.

GeFiCa – Germanium Field Calculator

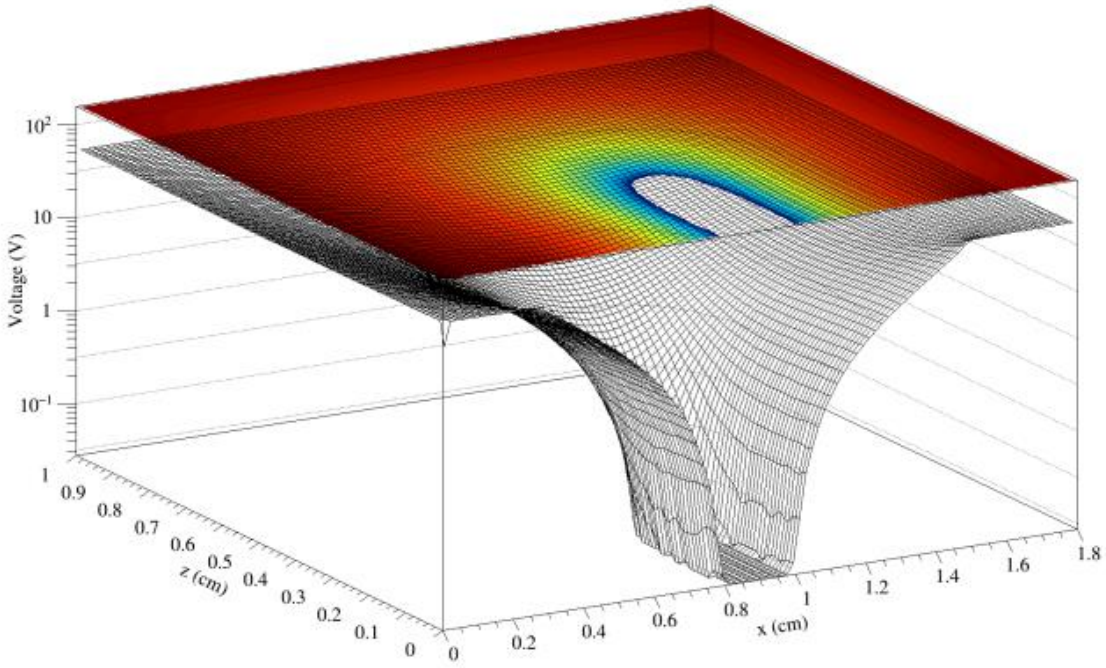

The potential field distribution in the detector when a positive voltage of 55 V was applied to the outside surface contact. The white area indicates that the detector is not fully depleted.

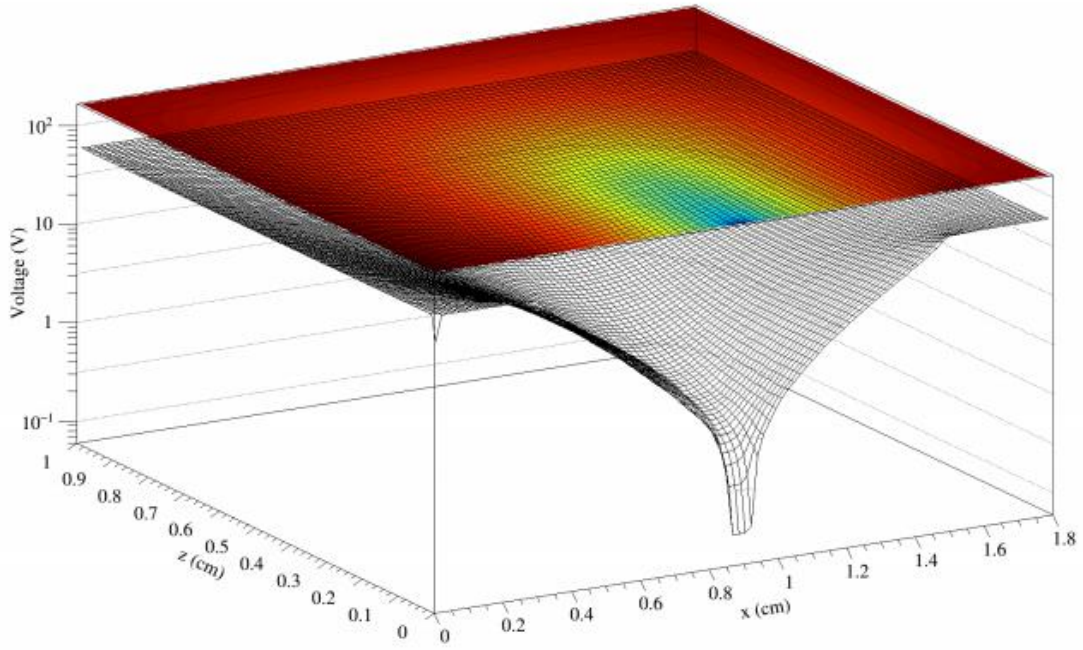

The potential field distribution in the detector when a positive voltage of 60 V was applied to the outside surface contact. The absence of any white area indicates that the detector is fully depleted.

- **GeFiCa** (Germanium Field Calculator), created by Dr. Liu and graduate students at USD to demonstrate analytic and numeric methods to calculate static electric fields and potentials in HPGe detectors.
- A planar geometry with the same dimensions as the real detector (except four wings where the electric field is expected to be extremely low) has been built in GeFiCa.

Potential and Electric Field Distribution at 400 V

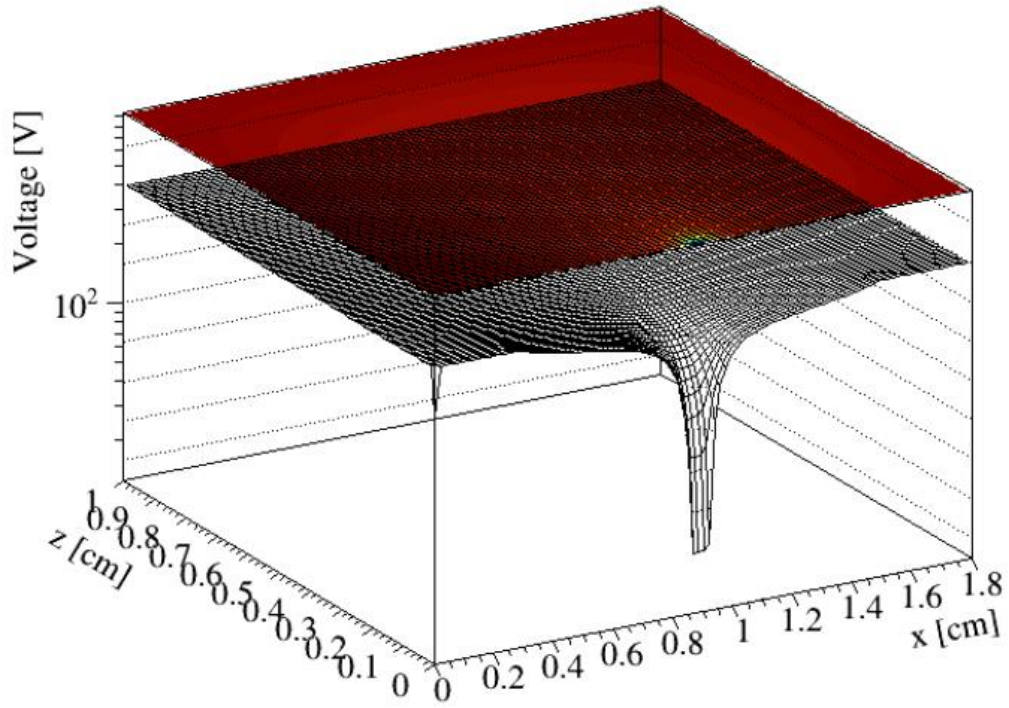

The potential field distribution in the detector when a positive voltage of 400 V was applied to the outside surface contact.

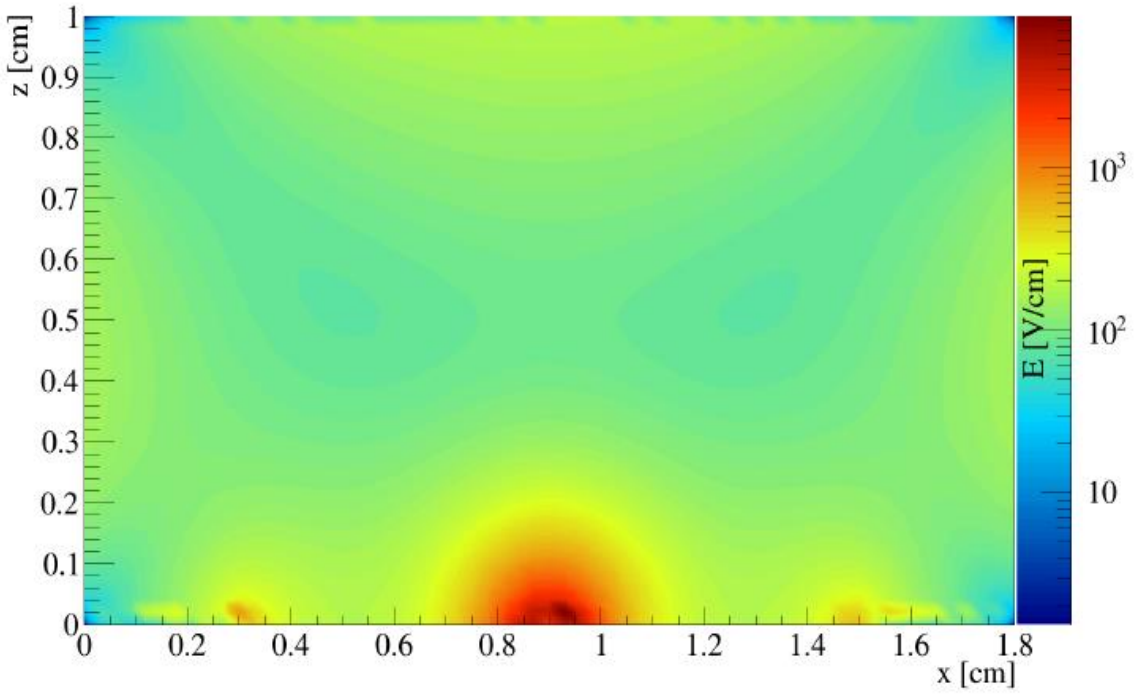

The electric field distribution in the detector when a positive voltage of 400 V was applied to the outside surface contact.

- The maximum electric field in the detector at 400 V is between 8,000 V/cm and 9,000 V/cm, which is significantly lower than the required minimum electric field of 15,000 V/cm for internal charge amplification to occur inside the detector. → **No internal charge amplification can be observed at 400 V**.

Expected Electric Field Distribution at 900 V

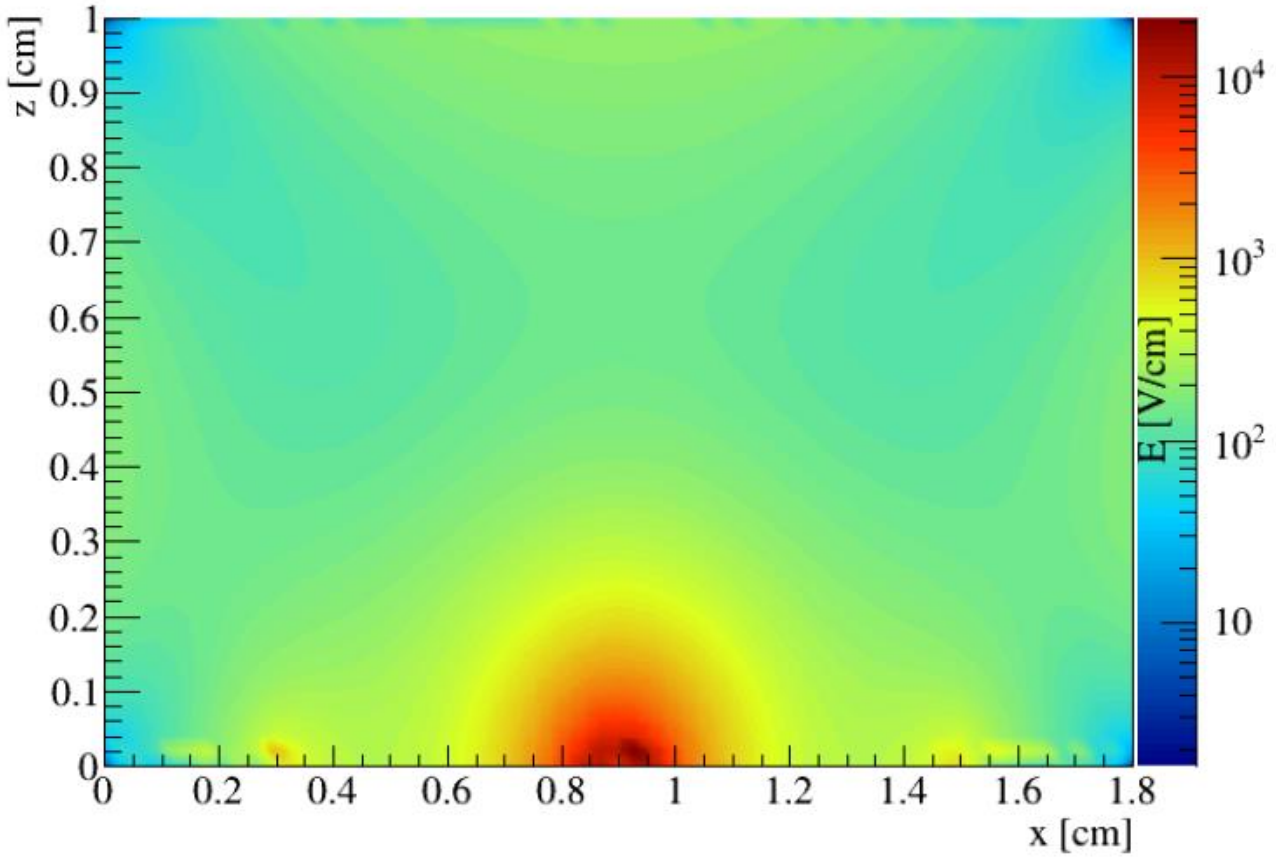

The electric field distribution in the detector when a positive voltage of 900 V was applied to the outside surface contact.

- Can reach 20,000 V/cm at 900 V → To observe the internal charge amplification with this detector, the applied voltage needs to be at least 900 V to reach the required electric field of 15,000 V/cm.
- Unfortunately, due to the fact that the leakage current of this detector jumped to a very high value starting from around 420 V because of field penetration into a-Ge, we were unable to apply the bias voltage beyond 400 V.

Future work:

- Optimize our fabrication process to improve the quality of the a-Ge contact to achieve the required electric field to observe the internal charge amplification.

*This study has been converted into a scientific paper and now is available in arXiv, please refer to **arXiv: 2105.02109** for more information.*

Geometry Design Simplification

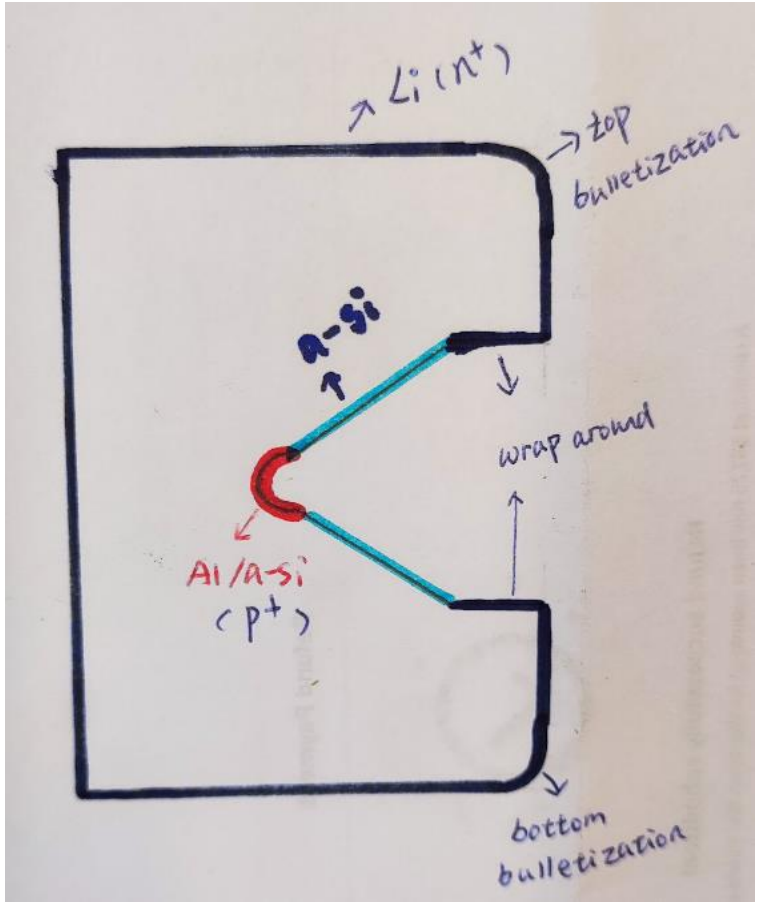

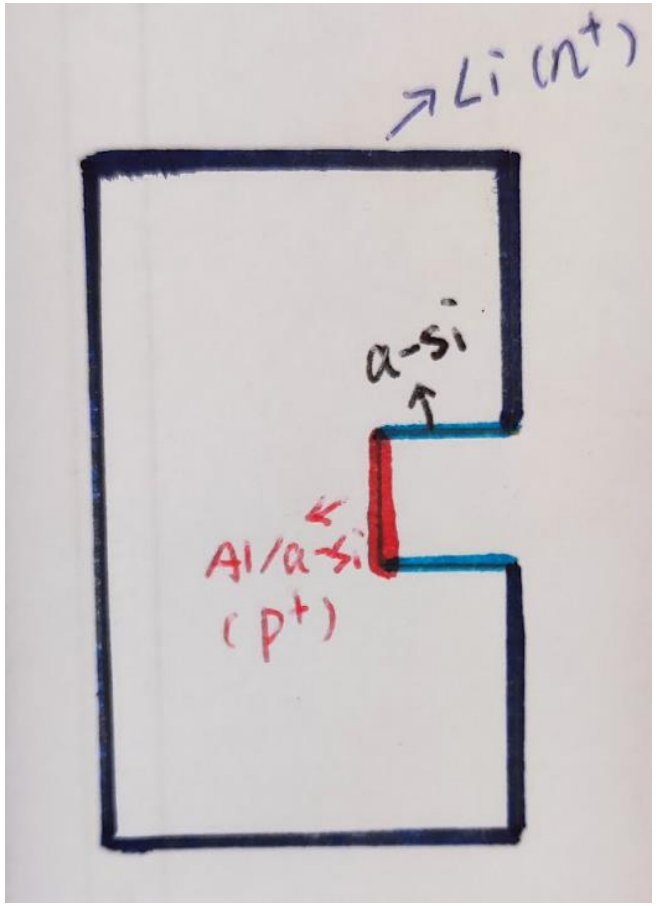

- ✓ Top and bottom bulletization
- ✓ Wrap around
- ✓ Ring contact bulletization
- ✓ Ring contact gap > ring contact length

- No bulletization for top and bottom (if no edge rounding device is available in TAMU)
- No wrap around
- No bulletization for ring contact
- Ring contact gap = ring contact length

Field Simulation from Siggen

Input:

1. Impurity concentration: (2.06 ~2.94) $\times 10^{10}/cm^3$
2. Applied bias voltage: 4000 V on the n+ contact.
3. The same height and radius as the real crystal.
4. Hole diameter: 20 mm

Output from Siggen:

```
  >>  Calculated capacitance at 4000 V: 28.639 pF
Writing weighting potential to file fields/wp_usd.dat
Estimated depletion voltage (or pinch-off?) = 3729 V
Minimum bulk field = 356.9 V/cm at (r,z) = (25.5, 25.0) mm
```

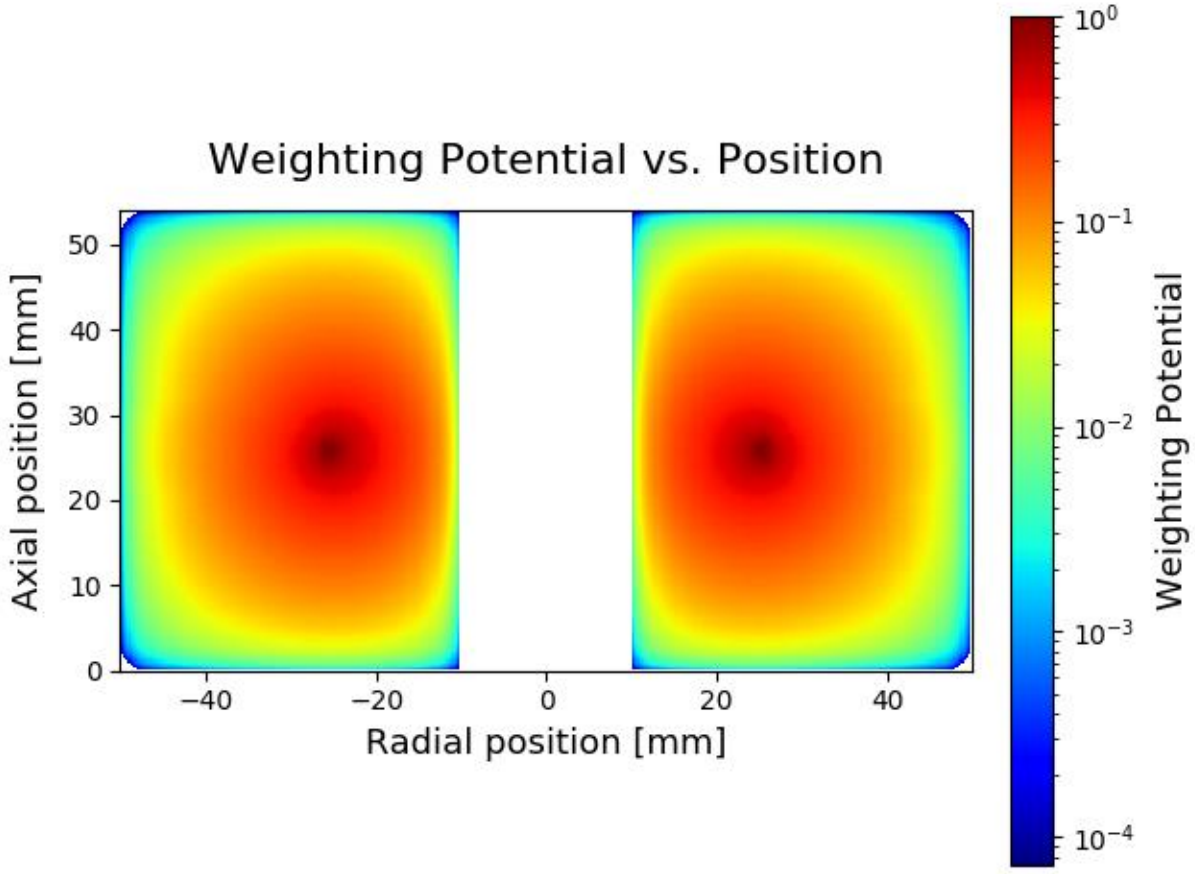

Weighting Potential

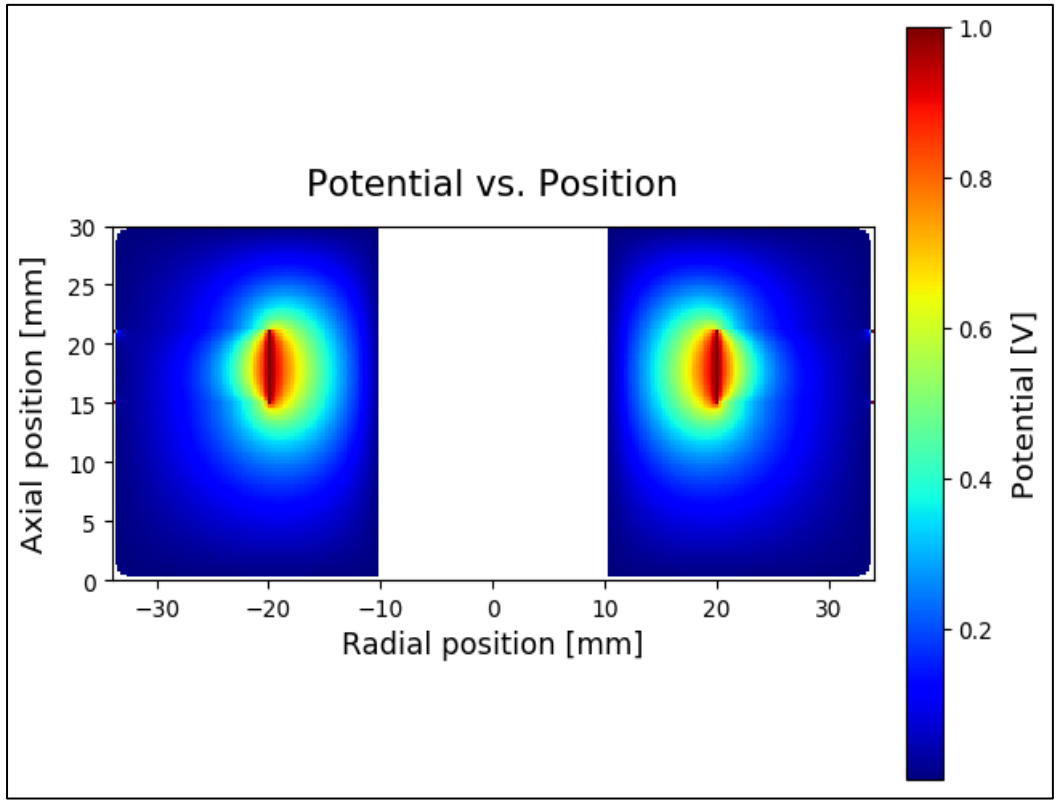

Crystal #1

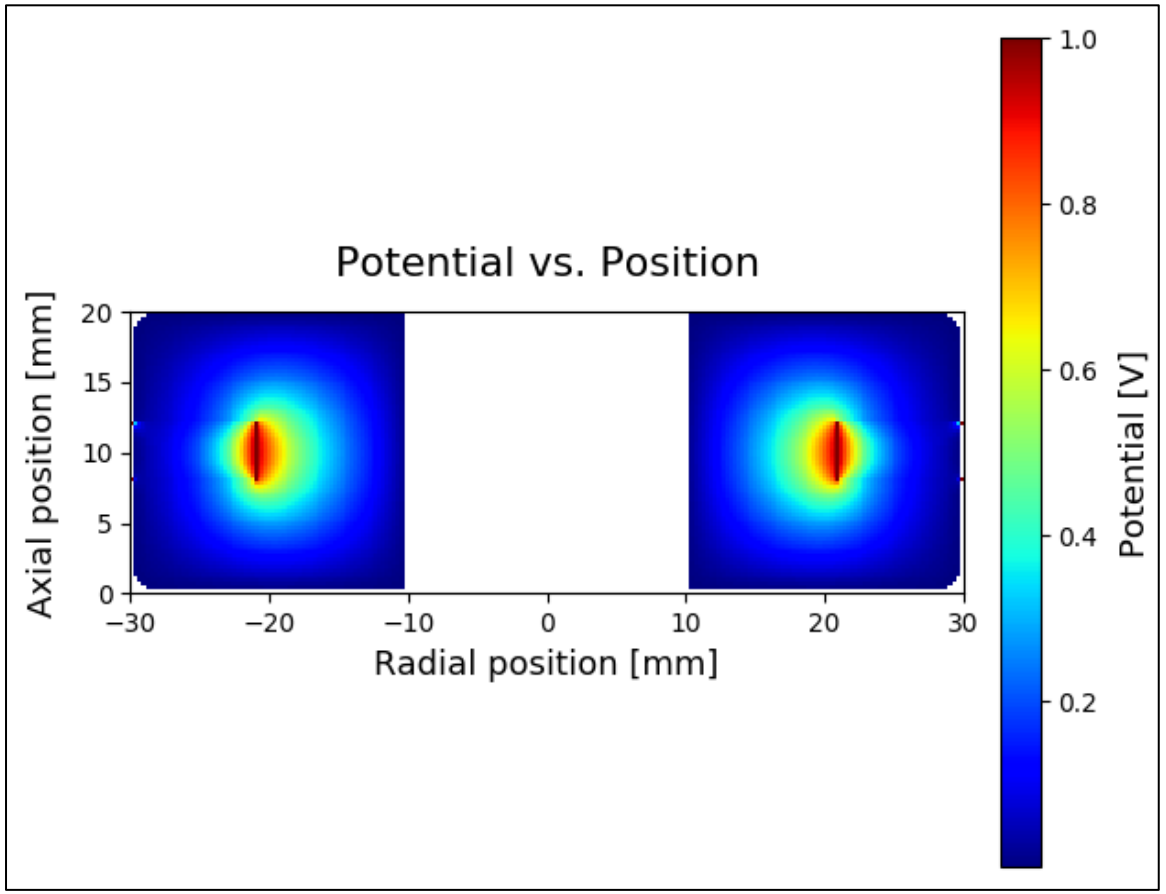

Crystal #2